*An earlier version of this work appears as part of a paper by W. P. Reinhardt and T. S. Murtaugh, in *Abstracts of the Seventh International Conference on the Physics of Electronic and Atomic Collisions* (North-Holland, Amsterdam, 1971), p. 221.

†NSF Predoctoral Fellow, Danforth Fellow.

[1]See, for example, R. G. Newton, *Scattering Theory of Waves and Particles* (McGraw-Hill, New York, 1966), Chap. 12; or, V. de Alfaro and T. Reggie, *Potential Scattering* (Interscience, New York, 1965).

[2]R. Jost and A. Pais, Phys. Rev. 82, 840 (1951).

[3]L. Schlessinger, Phys. Rev. 167, 1411 (1968); 171, 1523 (1968); and the review by R. W. Haymaker and L. Schlessinger, in *The Padé Approximant in Theoretical Physics*, edited by G. A. Baker, Jr. and J. L. Gammel (Academic, New York, 1970), Chap. 11.

[4]R. G. Newton, Ref. 1; J. Math. Phys. 2, 188 (1961).

[5]R. G. Newton, J. Math. Phys. 8, 2347 (1967).

[6]L. Schlessinger, Ref. 3; R. G. Newton, Ref. 1, p. 523.

[7]W. P. Reinhardt and A. Szabo, Phys. Rev. A 1, 1162 (1970).

[8]W. P. Reinhardt, Phys. Rev. A 2, 1767 (1970).

[9]See, for example, P. J. Davis, *Interpolation and Approximation* (Blaisdell, Waltham, Mass., 1963); J. R. Rice, *The Approximation of Functions* (Addison Wesley, Reading, Mass., 1964), Vol. 1.

[10]G. A. Baker, Jr., in *Advances in Theoretical Physics*, edited by K. A. Brueckner (Academic, New York, 1965), Vol. 1, p. 1. See also the review by G. A. Baker and J. G. Gammel, Ref. 3.

[11]H. S. Wall, *The Analytic Theory of Continued Fractions* (Van Nostrand, Princeton, N. J., 1948).

[12]K. Gottfried, *Quantum Mechanics* (W. A. Benjamin, New York, 1966), Vol. 1, Chap. 3.

[13]R. Blankenbecler, in *Strong Interactions and High Energy Physics*, edited by R. G. Moorehouse (Oliver and Boyd, Edinburgh, 1964).

[14]R. G. Newton, Ref. 6.

PHYSICAL REVIEW A VOLUME 5, NUMBER 2 FEBRUARY 1972

Effect of Charge Polarization on Inelastic Scattering: Differential and Integral Cross Sections for Excitation of the 2^1S State of Helium by Electron Impact*

James K. Rice
Sandia Laboratories, Albuquerque, New Mexico 87115

and

Donald G. Truhlar
Department of Chemistry, University of Minnesota, Minneapolis, Minnesota 55455

and

David C. Cartwright
Space Physics Laboratories, The Aerospace Corporation, El Segundo, California 90045

and

Sandor Trajmar
Jet Propulsion Laboratory, California Institute of Technology, Pasadena, California 91103

(Received 20 September 1971)

Experimental differential scattering cross sections for excitation of helium by electron impact from its ground state to its 2^1S state are presented at four incident electron energies in the range 26–55.5 eV for scattering angles between 10° and 70° and at 81.6 eV for scattering angles between 10° and 80°. These differential cross sections are normalized by using previously determined 2^1P cross sections and measured $2^1S/2^1P$ cross-section ratios. These experimental cross sections and cross-section ratios are compared with results predicted by the Born approximation, the polarized Born approximation, and several other first-order approximations in which direct excitation is calculated in the Born approximation and exchange scattering in various Ochkur-like approximations. Calculations based on these approximations are also compared to the data of other experimenters at energies up to 600 eV. The effect on the small-angle scattering of several nonadiabatic dipole-polarization potentials is examined. For the 34–81.6-eV energy range, it is shown that the inclusion of polarization is necessary for accurate predictions of the angle dependence of the 2^1S cross sections at small angles. Cross sections resulting from the use of analytic self-consistent-field wave functions for both the ground and excited states are presented. They agree well with those obtained from more accurate correlated wave functions.

I. INTRODUCTION

In many cases, the first Born approximation has been successful in explaining the differential cross sections for electronic excitation of atoms and molecules by electron impact at high energies (E greater than about 150 eV) and small scattering angles (less than about 15°).[1–5] This is the region

TABLE I. Measurements of the DCS's for the $1\,^1S \rightarrow 2\,^1S$ transition in helium.

Ref.	E (eV)	θ (deg)
9[a]	604	7.6–8.6
9[a]	511	3.8–8.8
9[a]	417	7.4–9.4
10[a]	500	4.7–15.3
11	500	0.5–2.5
14	50–400	5
2	300–400	5–10
2	150–225	5–15
2	100	5–20
12[b]	56.5	5–60
13[b]	22	20–145
Present	81.6	10–80
Present	26.5–55.5	10–70

[a]The $2\,^1S$ and $2\,^1P$ peaks were not completely resolved in all the spectra reported in these references.

[b]The cross sections are given in relative units.

where a study of the assumptions behind the first Born approximation leads us to expect it to be most valid, although the quantitative validity of the theory depends on the particular nature of the transition.[5,6] It is desirable to find a calculational scheme, as simple to apply as the first Born approximation, which represents the essential features of the scattering process at intermediate impact energies ($E \cong 15$–150 eV).

In a previous article[7] we presented a theoretical and experimental study of the electron-scattering differential cross sections (DCS's) for the $(1s^2)1\,^1S \rightarrow (1s2p)2\,^1P$ transition in helium. In that paper we show that the experimentally measured angle dependence of the DCS for $\theta \lesssim 40^\circ$ and $E = 34$–82 eV agrees well with that predicted by the first Born approximation, which neglects the effects of electron exchange, distortion of the scattering-electron wave function, and polarization of the target by the incoming electron. In the present article we use similar methods to study the $(1s^2)1\,^1S \rightarrow (1s2s)2\,^1S$ transition. We find, however, that it is necessary to include polarization of the target, and we use the polarized Born approximation (a first Born calculation augmented by polarization)[8] to explain the experimental data. We again show that it is not necessary to treat exchange and distortion accurately to explain the main features of the angular dependence of the small-angle DCS. We discuss experimental and theoretical results for the ratios of the cross sections for these two excitations and for both the differential and integral cross sections for excitation of the $2\,^1S$ state.

The previous DCS studies[2,9–14] of the $2\,^1S$ state are limited to small scattering angles $\theta \leq 20^\circ$ (except for energies near threshold and for the data of Ref. 12 which are in error at large θ due to double scattering[15]). These studies are summarized in Table I, where they are compared with the present experimental conditions. There are several previous experimental determinations of the $2\,^1S/2\,^1P$ DCS ratios.[16–26] These are summarized in Table II, where the energy and angular ranges are compared to the present work. By using our experimental cross-section ratios and our approximate normalization of the $2\,^1P$ DCS's (Ref. 7) we can put our $2\,^1S$ DCS's on an absolute scale. Further, we integrate our $2\,^1S$ DCS's to obtain experimental estimates of the absolute $2\,^1S$ integral cross sections for impact energies $E = 26.5$–81.6 eV. The only previous experimental estimates of this quantity were obtained by Dugan, Richards, and Muschlitz[27] for $E = 25$–135 eV and by Vriens, Simpson, and Mielczarek[2] for $E = 100$–400 eV.

Kim and Inokuti[5] concluded from a study of the available low-angle data in the 200-400-eV incident-energy range that the Born approximation is valid down to lower energies for excitation of the $2\,^1P$ state than it is for excitation of the $2\,^1S$ state. We study this question further in this paper. Moiseiwitsch and Smith[28] pointed out that the Born-Oppenheimer approximation, which includes exchange effects, is much worse for $S \rightarrow S$ transitions than for $S \rightarrow P$ transitions. This fault occurs because the Born-Oppenheimer approximation greatly overestimates the effect of exchange for the former case. We bypass this difficulty by accounting for exchange using several Ochkur-like theories.[7,29–37] These theories give more reasonable predictions for the magnitude of the exchange effect and show that for qualitative purposes we

TABLE II. Measurements of the DCS ratios $2\,^1S/2\,^1P$.

Ref.	E (eV)	θ (deg)
23	25 000	0
9	511	4.0–8.8
10	500	6.3–15.3
11	500	0.5–2.5
2	300–400	5–10
17	235	9
2	150–225	5–15
18	202	0
2	100	5–20
19	22–80.8	0
12	56.5	5–60
16	50	0
24	48 and 500	0–12
25	48	0–12
22	46	90
14	50–400	5
26	30–50	5–100
Present	81.6	10–80
Present	26.5–55.5[a]	0–70

[a]Some of these results were presented in a preliminary communication (Ref. 83).

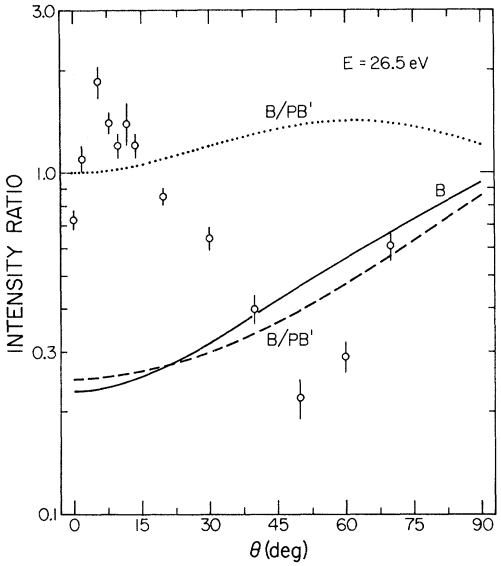

FIG. 1. Ratio of DCS of the $1\,^1S \rightarrow 2\,^1S$ transition to that of the $1\,^1S \rightarrow 2\,^1P$ transition as a function of scattering angle θ for $E = 26.5$ eV. The circles (with error bars) are the present experimental results and the curves are calculated by the indicated method. The dotted line was obtained with $b = (\frac{5}{4})\, b_1^{\mathrm{FW}} = 1.93 a_0$ and the dashed line with $b = 2(\frac{5}{4})\, b_1^{\mathrm{FW}} = 3.86 a_0$. The value of α is $1.584 a_0^3$ in both cases.

may neglect exchange at small scattering angles.

II. EXPERIMENTS

The electron-impact spectrometer and data-collection procedures used to obtain the experimental results reported here have been described previously in Ref. 7.

The basic experimental measurements consist of the determination of the intensity of electrons scattered after losing an energy corresponding to excitation of the $2\,^1S$ state relative to the intensity resulting from excitation of the $2\,^1P$ state as a function of scattering angle for a fixed incident energy. These intensity measurements were taken from the same energy-loss spectra used to obtain much of the data presented in Ref. 7. The $2\,^1S/2\,^1P$ intensity ratios are determined by dividing the height of the $2\,^1S$ energy-loss peak by that of the $2\,^1P$ peak at each angle and energy ($0° \leq \theta \leq 70°$ for $E = 26$, 34, 44, and 55.5 eV and $10° \leq \theta \leq 80°$ for $E = 81.6$ eV). Peak heights rather than areas can be used since the peak shapes were found to be independent of scattering angle. The instrumental factors relating the peak intensities to their respective DCS's are the same, to a good approximation, for both the $2\,^1S$ and the $2\,^1P$ energy-loss features in any one spectrum; therefore, these intensity ratios equal the corresponding DCS ratios. These experimentally determined ratios are shown in Figs. 1–3 along with the results of several theoretical calculations which are discussed in Secs. III and IV. The error limits assigned to these ratios, except at 81.6 eV, are the average deviations of 4–7 determinations at each angle. Each 81.6-eV datum represents a single determination.

The $2\,^1S/2\,^1P$ (and $2\,^3S/2\,^1P$, $2\,^3P/2\,^1P$, and $3\,^3S/2\,^1P$) intensity ratios at $\theta = 0°$ agree well with those of Chamberlain, Heideman, Simpson, and Kuyatt[19] at $E = 55.5$, 44, and 34 eV but disagree with theirs at $E = 26$ eV. Since a change in our E of + 0.5 eV (which is within our uncertainty in E, see Ref. 7) completely resolves this discrepancy, we shall assume that $E = 26.5$ eV in this case.

The absolute $2\,^1S$ DCS's are computed from the above intensity ratios and the renormalized absolute $2\,^1P$ DCS's from Ref. 7 as discussed below. The extrapolation procedure used in Ref. 7 to facilitate normalization of the $2\,^1P$ DCS's assumed

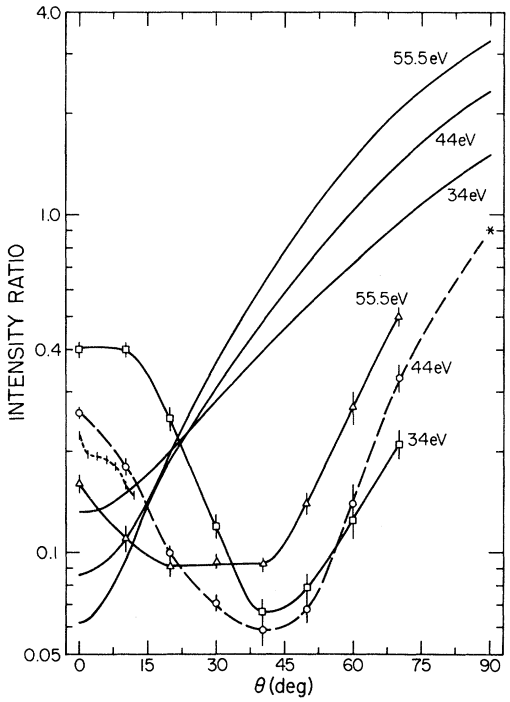

FIG. 2. Ratio of DCS of the $1\,^1S \rightarrow 2\,^1S$ transition to that of the $1\,^1S \rightarrow 2\,^1P$ transition as a function of scattering angle θ. The present experimental results at $E = 55.5$ (triangles with error bars and connected by a solid curve), 44 (circles with error bars and connected by a dashed curve), and 34 eV (squares with error bars and connected by a solid curve); the results of Lassettre, Skerbele, Dillon, and Ross (Ref. 25) at $E = 48$ (short-dashed curve) and a value from Doering (Ref. 22) at 46 eV (asterisk) are shown. The monotonic solid curves are calculated at 34, 44, and 55.5 eV in the Born approximation.

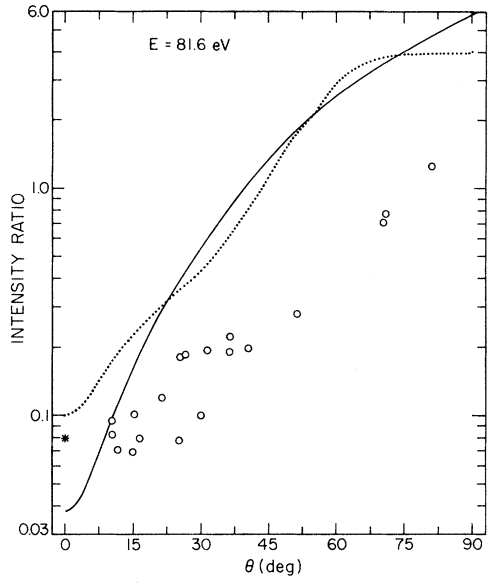

FIG. 3. Same as Fig. 1 except that $E = 81.6$ eV. The circles are the present experimental results; the asterisk is the 0° result of Chamberlain, Heideman, Simpson, and Kuyatt (Ref. 19) at $E = 80.7$ eV. The solid curve is calculated in the Born approximation (B) and the dotted curve in the polarized Born approximation (B/PB′) with $\alpha = 1.584 a_0^3$ and $b = \frac{5}{4} b_1^{\mathrm{FW}} = 3.39 a_0$.

that the cross sections decrease monotonically with increasing angle. However, close-coupling calculations of electron–hydrogen-atom $1s$-$2p$ scattering predict DCS's which rise significantly at high angles.[38] Consequently, we renormalized the $2\,^1P$ DCS's presented in Ref. 7 by assuming a constant cross section for angles greater than those for which data were obtained. These renormalized values are lower than those of Ref. 7 by 1.6% at $E = 81.6$ eV, by 7.6% at $E = 55.5$ eV, by 8.0% at $E = 44$ eV, by 7.8% at $E = 34$ eV, and by 19.5% at $E = 26.5$ eV. The normalized experimental $2\,^1S$ DCS's are presented in Figs. 4–8, along with the results of several theoretical calculations which are discussed in Secs. III and IV.

The error bars assigned to the $2\,^1S$ DCS data include the error in the ratios and uncertainties in the shape of the $2\,^1P$ DCS's and, therefore, include the uncertainty in the angular dependence of the $2\,^1S$ DCS's but only part of the uncertainty in their magnitude. The percentage uncertainty in the over-all scale at each energy is approximately equal to the "estimated percent error" in the integral of the $2\,^1P$ DCS's given in Table II of Ref. 7.

The $2\,^1S$ integral cross section $Q(E)$ is related to the DCS $I(E, \theta)$ by

$$Q(E) = 2\pi \int_0^{\pi} I(E, \theta) \sin\theta \, d\theta \quad . \tag{1}$$

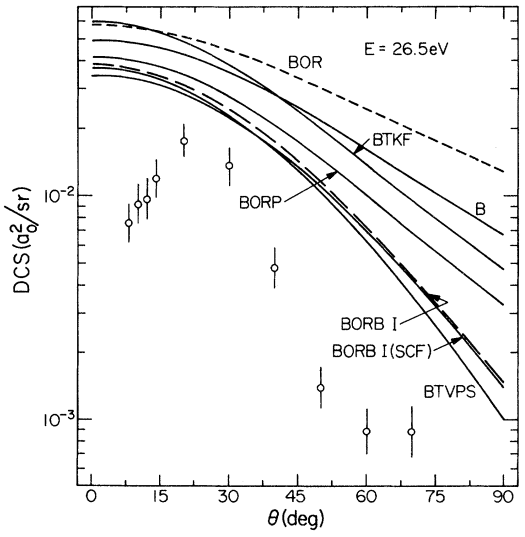

FIG. 4. DCS vs scattering angle for $E = 26.5$ eV. The circles (with error bars) are the present experimental results. The curve labeled BORB I(SCF) is calculated in the symmetrized Born-Ochkur-Rudge approximation with the SCF wave functions. The other curves are calculated in the indicated approximations using the accurate generalized oscillator strengths (Refs. 5 and 75).

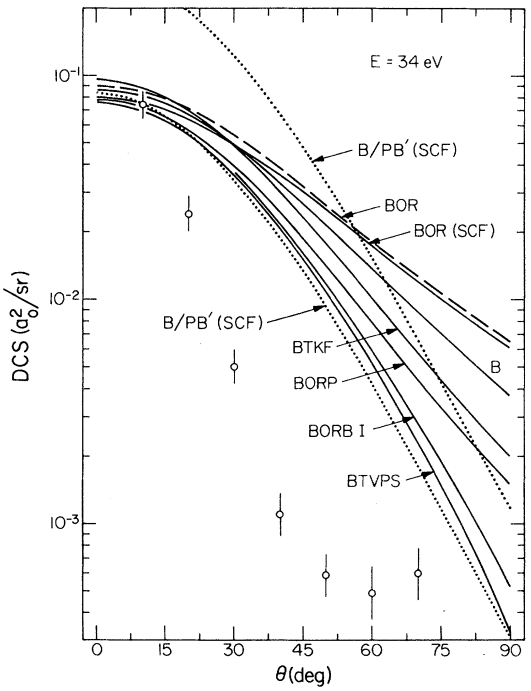

FIG. 5. DCS vs scattering angle θ for $E = 34$ eV. The circles (with error bars) are the present experimental results. The curves are calculated using the accurate generalized oscillator strengths (Refs. 5 and 75). The upper dotted curve is calculated in the polarized Born approximation with $\alpha = 1.584 a_0^3$ and $b = \frac{5}{4} b_1^{\mathrm{FW}} = 2.19 a_0$. The lower dotted curve is the same but renormalized to experiment at $\theta = 10°$. No other calculation is renormalized.

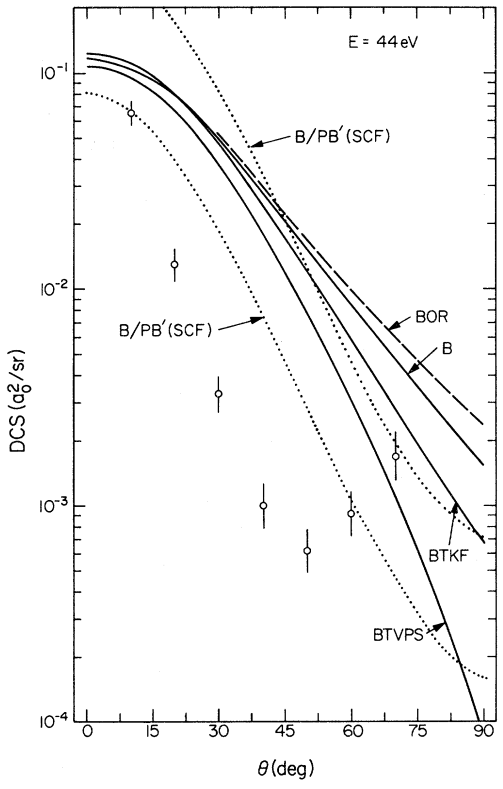

FIG. 6. Same as Fig. 5 except $E = 44$ eV and $b = 2.49a_0$.

In order to perform this integration, the $2\,^1S$ DCS's are extrapolated to 0° and to 180°. The extrapolation to 0° introduces little uncertainty into the integral (see Ref. 7) but the extrapolation to 180° is subject to large uncertainties since the $2\,^1S$ DCS's are generally rising at the highest angles for which data are obtained. The contribution to Eq. (1) of the extrapolation to 180° is assumed to be

$$Q_{\text{ext}}(E) = 2\pi I(E, \theta_{\max}) \int_{\theta_{\max}}^{\pi} \sin\theta \, d\theta \quad , \tag{2}$$

where $\theta_{\max}$ is the largest angle for which data are obtained. Table III gives the contributions to $Q(E)$ from angles less or greater than $\theta_{\max}$ and the resulting $2\,^1S$ integral cross sections. The estimated percent error given in this table includes contributions from both regions of the integral and includes the uncertainty in both the shape and scale of the $2\,^1S$ DCS's.

TABLE III. Integration of the $2\,^1S$ DCS's to obtain integral cross sections $Q(10^{-2}a_0^2)$.

		Contributions to Q			
E (eV)	$\theta_{\max}$ (deg)	$\theta \le \theta_{\max}$	$\theta \ge \theta_{\max}$	Q	Estimated % error
26.5	70	2.2	0.7	2.9	50
34	70	2.8	0.4	3.2	35
44	70	2.5	1.5	4.0	48
55.5	70	2.6	3.0	5.6	52
81.6	80	2.5	0.9	3.4	58

III. THEORY

A. Scattering Equations

Many aspects of the theory of electron scattering by the helium atom are well developed.[4,28,39,40] In particular, the channel wave functions $F_{\gamma 1}^{LS}(r)$ in the expansion in atomic eigenstates method satisfy coupled equations of the form[41,42]

$$\frac{1}{2}\left(\frac{d^2}{dr^2} - \frac{l_\gamma(l_\gamma+1)}{r^2} + k_\gamma^2\right) F_{\gamma 1}^{LS}(r) = \sum_{\gamma'=1}^{N} V_{\gamma\gamma'}(r) F_{\gamma' 1}^{LS}(r) \quad , \tag{3}$$

where L and S are the total orbital- and spin-angular-momentum quantum numbers, respectively, r is the separation between the scattering electron and the atomic nucleus, γ denotes the state of the atom, k_γ is the wave number of the electron when the atom is in state γ, l_γ is the relative orbital-angular-momentum quantum number of the electron, the subscript 1 denotes the ground state ($1\,^1S$) of the helium atom, $V_{\gamma\gamma'}$ are matrix elements of the (nonlocal) effective potential V, and the sum

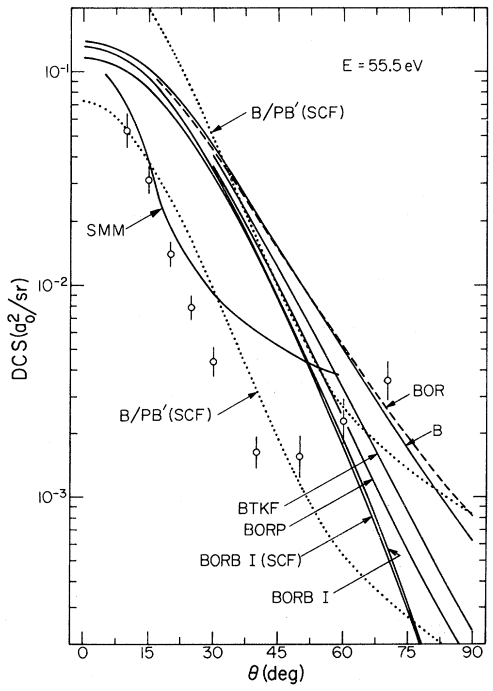

FIG. 7. Same as Fig. 5 except $E = 55.5$ eV and $b = 2.79a_0$. The curve labeled SMM is an experimental result from Ref. 12 (56.5 eV) and is normalized to the lower dotted curve at 30°.

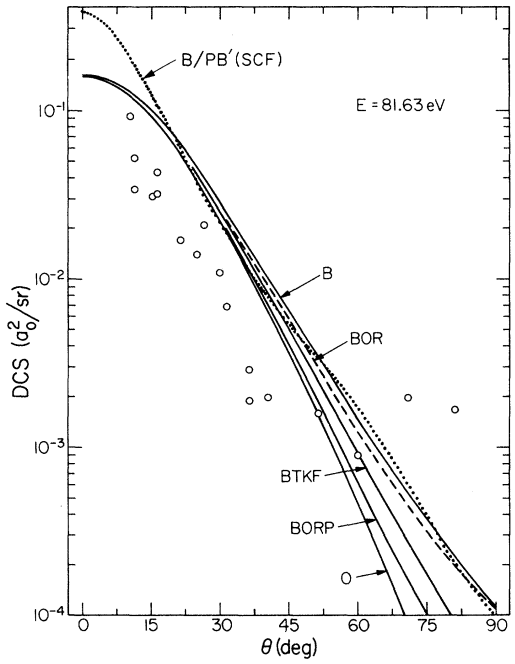

FIG. 8. Same as Fig. 5 except $E = 81.6$ eV, $b = 3.39a_0$, all the data are shown (circles without error bars), and no renormalized calculations are presented.

is over all atomic eigenstates γ' in the (necessarily truncated) expansion of the wave function. For a particular transition we may obtain an approximate solution to Eq. (3) by truncating the atomic-state expansion at two states and including the effects of the omitted states by adding to V an approximate generalized optical potential U.[41,43] A first-order approximation to the transition amplitude is then obtained by taking the matrix elements of $(V+U)_{\gamma\gamma'}$ between plane-wave approximations to the channel wave functions. The scattering amplitude can be written

$$f_{\gamma\gamma'} = f^{\mathrm{BO}}_{\gamma\gamma'} + f^{P}_{\gamma\gamma'} \quad ,$$

where $f^{\mathrm{BO}}_{\gamma\gamma'}$ is the Born-Oppenheimer[44] amplitude due to scattering by $V_{\gamma\gamma'}$ and $f^{P}_{\gamma\gamma'}$ is the polarization amplitude due to scattering by $U_{\gamma\gamma'}$. In order to eliminate some of the special problems in $f^{\mathrm{BO}}_{\gamma\gamma'}$ due to difficulties in making a first-order approximation for the exchange scattering,[36] we will usually substitute the Born approximation for the Born-Oppenheimer approximation, i.e., neglect the exchange contributions to $f^{\mathrm{BO}}_{\gamma\gamma'}$. To test the validity of this procedure, we have computed some cross sections using Ochkur-like methods which approximately correct the Born (B) approximation for exchange scattering. The methods include the prior form of the Ochkur (O), the prior form of the Born-Ochkur-Rudge (BOR), the post form of the Born-Ochkur-Rudge (BORP), the symmetrized Born-Ochkur-Rudge (BORB I), the Born-transferred Kang-Foland (BTKF), and the Born-transferred Vainshtein-Presnyakov-Sobelman (BTVPS) approximations. These methods have been discussed with appropriate references in Ref. 7 and the reader is referred there for details. Calculations which neglect the polarization potential U, i.e., approximate $f_{\gamma\gamma'}$ by setting $f^{P}_{\gamma\gamma'} = 0$, will be called static approximation calculations.

For the $1\,^1S \rightarrow 2\,^1P$ transition, the direct local part of $V_{\gamma\gamma'}$ has the form[45]

$$V_{\gamma\gamma'}(r) \sim O(r^{-2}), \quad \text{large } r \quad . \tag{4}$$

This is a long-range potential and should dominate small-angle scattering. Thus, the successes[2,7] of the static approximation for the treatment of small-angle scattering involving the $1\,^1S \rightarrow 2\,^1P$ transition should not be surprising.

For the optically forbidden $1\,^1S \rightarrow 2\,^1S$ transition, however, the static approximation potential V has the asymptotic form[45]

$$V_{\gamma\gamma'} \sim O(e^{-cr}), \quad \text{large } r \tag{5}$$

where $c > 0$. Since this is such a short-range potential, we must examine the asymptotic behavior of $U_{\gamma\gamma'}$ to determine the dominant contributor to small-angle scattering.

The long-range behavior of $U_{\gamma\gamma'}$ can be obtained in the adiabatic approximation,[46-50] which assumes that fluctuations in the incident particle's kinetic energy are small compared to fluctuations in the energy of the target (virtual excitations).[46-48,51,52] When the adiabatic approximation is made in the initial state (electron in the field of helium in its $1\,^1S$ state), the polarized Born transition amplitude is calculated using $V_{12} + U_{12}$. When the adiabatic approximation is made in the final state (electron in the field of helium in its $2\,^1S$ state), the polarized Born transition amplitude is calculated using $V_{12} + U_{21}$. The generalized optical potential has the asymptotic form

$$U_{ij} \underset{r\to\infty}{\sim} \alpha_{ij}/2r^4 \quad , \tag{6}$$

where

$$\alpha_{ij} = 2\textstyle\sum_n Z_{in} Z^*_{jn}/(E_n - E_i) \quad .$$

The sum over n is over all $n\,^1P$ states (and includes an integration over the continuum). E_γ is the energy of atomic state $\gamma(i\,^1S,\ j\,^1S,\ \text{or } n\,^1P)$ and

$$Z_{in} = \langle i\,^1S \,|\, z_1 + z_2 \,|\, n\,^1P \rangle \quad .$$

The quantities z_1 and z_2 are the z components of the position vectors of the two electrons on the helium atom.

Any of the standard techniques of perturbation theory can be applied to evaluate α_{ij}; that is, we could use direct summation of the expression re-

sulting from an expansion in unperturbed eigenfunctions, the Z^{-1} expansion,[53,54] or Buckingham's variational-perturbational method for obtaining first-order perturbed functions.[55-58] The variation-perturbation method has the advantage that it can be used to compute very accurate values of the transition polarizabilities. Drake[59] has applied this method to obtain the static transition polarizabilities using 50-term correlated wave functions. The construction of the basis sets used for his calculation is described by Drake and Dalgarno.[60] Drake finds $\alpha_{21} = 101.6a_0^3$ and $\alpha_{12} = 1.584a_0^3$.

Even in the adiabatic approximation, the asymptotic form [Eq. (6)] is not valid at all r, and we use the two-parameter forms

$$U_{ij}^{A} = -\alpha_{ij}/2(r^2+b^2)^2 \ , \tag{7}$$

$$U_{ij}^{B} = \begin{cases} -\alpha_{ij}/2r^4, & r > b \quad (8) \\ -\alpha_{ij}/2b^4, & r \leq b \quad (9) \end{cases}$$

$$U_{ij}^{B'} = \begin{cases} -\alpha_{ij}/2r^4, & r > b \quad (10) \\ -\alpha_{ij}r/2b^5, & r \leq b \quad (11) \end{cases}$$

$$U_{ij}^{C} = \begin{cases} -\alpha_{ij}/2r^4, & r > b \quad (12) \\ 0 \ , & r \leq b \quad (13) \end{cases}$$

as approximate representations of the transition polarization potential for all r. The forms are chosen so that by making b large we can reduce the polarization potential for $r < b$ from its asymptotic form. Increasing the value of b can also simulate the main nonadiabatic effect, which is a further reduction in the potential from its adiabatic form. In this regard the form B', which has not been used previously, is apparently the most realistic[61] of the four.

The scattering amplitude in the polarized Born approximation (B/PX) is

$$f^{B/P} = f^{B} + f^{P} \tag{14}$$

and in the polarized Born-Ochkur-Rudge approximation (BOR/PX) is

$$f^{BOR/P} = f^{BOR} + f^{P} \ , \tag{15}$$

where f^{B} and f^{BOR} are the usual Born and Born-Ochkur-Rudge scattering amplitudes,[7] f^{P} is the scattering amplitude calculated using the transition polarization potentials given by Eqs. (7)–(13), and $X = A, B, B'$, or C to denote the form of the polarization potential used in the calculation. U_{ij} and f^{B} depend on the phases of the bound-state functions in the same way; thus, the polarized Born cross sections (proportional to the squared modulus of $f^{B/P}$) will be independent of the phases of the bound-state wave functions. We choose the spatial part of the $1\,^1S$ bound-state wave function positive. The spatial part of the $2\,^1S$ bound-state wave function is chosen negative at the nucleus and positive at large r_1 and r_2. In this case f^{B} is positive for all scattering angles θ, and α_{ij} is positive when evaluated theoretically. The transition polarization potential U_{ij} is spherically symmetric, and thus f^{P} can be obtained analytically for the potentials of Eqs. (7)–(13).

The scattering amplitude associated with U_{ij}^{A} is positive for all θ. The scattering amplitudes associated with the B, B', and C forms of the polarization potential may be positive or negative, depending on θ. However, since all four forms lead to f^{P} being positive at small θ, the polarization amplitude will interfere constructively with f^{B} there and will increase the small-angle scattering. Since the form of f^{P} for large θ depends on the uncertain details of the small-r form of $U_{ij}(r)$, we cannot trust the predictions of this simple polarization model at large scattering angles. By using more than one small-r form for U_{ij}, we get an estimate of how large a scattering angle can be treated without a better model for the polarization potential.

Previous treatments of the polarization effect indicate that α_{ij} should be independent of energy and equal to the static transition polarizability but that the cutoff parameter b in Eqs. (7)–(13) should be energy dependent. Mittleman[62] discussed the polarization effect for inelastic scattering and concluded that nonadiabatic effects may be larger in this case than for elastic scattering, i.e., b may be very large.

There are at least two reasons why we might expect nonadiabatic effects to be larger for electronically inelastic scattering than for electronically elastic scattering. (i) A change of electronic state is a nonadiabatic phenomenon. (ii) Elastic scattering is dominated by large l_2 (large impact parameters in semiclassical language). At any given energy, the relative velocity along the line connecting target and projectile is smaller for larger impact parameters than it is for smaller ones. Consequently, electronic adiabaticity (which roughly depends on the relative velocity being smaller than the average kinetic energy of the bound electrons) is more likely when l_2 is large. Inelastic-scattering cross sections are smaller than elastic-scattering cross sections, so that they depend more on low-partial-wave scattering; thus, the adiabatic approximation should not be as accurate for inelastic scattering as for elastic scattering.

Polarization corrections must become small at very high energies. Nevertheless, in treating electronically elastic scattering, it has been found that use of the static polarizability and a value for the cutoff about equal in magnitude to that of the target dimensions provides a reasonable approximation even at energies as high as 700 eV.[8,63-65] Holt and Moiseiwitsch's[66] second Born calculations

TABLE IV. Values of the cutoff parameter b_j^{FW} computed using the Fetter-Watson formula [Eq. (16)].

E (eV)	k_1 (a_0^{-1})	k_2 (a_0^{-1})	b_1^{FW} (a_0)	b_2^{FW} (a_0)
26.50	1.40	0.66	1.54	29.72
44.00	1.80	1.31	1.99	59.24
81.63	2.45	2.12	2.71	95.69
150.00	3.32	3.08	3.67	139.35
300.00	4.70	4.53	5.20	204.77
500.00	6.06	5.94	6.71	268.23
25 000.00	42.87	42.85	47.43	1836.24

show that polarization corrections become small at a lower energy for inelastic scattering than for elastic scattering.

As shown above, we obtain different adiabatic polarization potentials if we consider polarizing interactions in the initial and final states. Since we do not have a good method for quantitatively estimating nonadiabatic effects, we wish to use the case which has smaller nonadiabatic corrections. Fetter and Watson[51] (FW) show that a reasonable criterion for validity of the adiabatic approximation in state j for an electron with wave number k_j at a distance r much greater than the atomic radius is

$$b_j^{FW} \equiv k_j/\langle \Delta E_j^n \rangle \ll r \quad . \tag{16}$$

In Eq. (16), $\langle \Delta E_j^n \rangle$ is the effective average value of ΔE_j^n, the energy difference between state $n\,^1P$ and state $j\,^1S$, over all $n\,^1P$ states causing polarization. The usual approximation is $\langle \Delta E_j^n \rangle \cong U_j$, where U_j is the ionization potential in state j. In our case, $U_1 = 0.90372$ a.u. and we take $\langle \Delta E_1^n \rangle = U_1$. We note that excitations from the $2\,^1S$ state are dominated by those to the $2\,^1P$ state. Thus, rather than using $U_2 = 0.14597$ a.u. for an estimate of $\langle \Delta E_2^n \rangle$, we use the $2\,^1P - 2\,^1S$ energy difference, i.e., $\langle \Delta E_2^n \rangle \cong \Delta E_2^2 = 0.02213$ a.u. We can now use b_j^{FW} as an estimate of b (we expect that b is at least approximately proportional to b_j^{FW} with an energy-independent constant of proportionality). The results are shown in Table IV. The table shows that the adiabatic approximation to polarizing interactions in the final state is a good approximation only for distances too large to be interesting. However, it also shows that we can use the adiabatic approximation to polarizing interactions in the initial state to obtain a useful estimate of the polarization effect. For lack of a better theory at this time, we will use $\alpha \equiv \alpha_{ij} = \alpha_{12}$, and we will consider b_1^{FW} to be the theoretically most justified choice for b in Eqs. (7)–(13).

At zero momentum transfer, the scattering amplitudes f^P associated with the polarization forms A, B, B', and C are $\pi\alpha/4b$, $4\alpha/3b$, $5\alpha/4b$, and α/b, respectively. In order to make these amplitudes equal for zero momentum transfer, we use $b = (\text{const}) \times b_1^{FW}$, where the constant is $\frac{1}{4}\pi$, $\frac{4}{3}$, $\frac{5}{4}$, and 1 for forms A, B, B', and C, respectively. We will also consider an empirical determination of b in Sec. IV A 1.

B. Wave Functions

Many approximate wave functions for the $1\,^1S$ ground state of helium have been reported in the literature. Calculations based on two of these wave functions are presented here. One of these is the 53-term correlated wave function of Weiss.[67] The other is Clementi's[68] self-consistent-field (SCF) double-ξ Hartree-Fock function

$$\Psi_1 = \xi_0(\vec{r}_1)\,\xi_0(\vec{r}_2)\,\eta(1,2) \quad . \tag{17}$$

In Eq. (17), η is a singlet spinor,

$$\xi_0(\vec{r}_k) = \sum_{i=1}^{2} c_{0i}\,\chi_{0i}(r_k) \quad , \tag{18}$$

and $\chi_{0i}(r)$ is a normalized hydrogenic $1s$ orbital with orbital exponent Z_{0i}. The coefficients c_{0i} and orbital exponents are given in Table V. These two wave functions are compared with each other and with some others in Table VI. For first-order scattering theories, the spatial extent of the electron-charge distribution is of primary importance in determining the accuracy of the calculated cross sections.[69,70] Therefore, as an additional check on the accuracy of the calculations to be presented in Sec. III C, the expectation value $\langle r_1^2 + r_2^2 \rangle$ is also included in Table VI. Comparison with the "exact" results of Pekeris[71] shows that the Clementi wave function is quite accurate, at least for this expectation value.

The calculations presented here which use the Weiss $1\,^1S$ wave functions also employ his $2\,^1S$ wave function.[67] To find a $2\,^1S$ wave function to use with Clementi's[68] SCF $1\,^1S$ wave function, we consider the orbital approximation[72]

TABLE V. Parameters for the self-consistent-field (SCF) wave functions.

State	n	i	c_{ni}	Z_{ni} [a]
$1\,^1S$ [b]	0	1	0.835188	1.446
	0	2	0.189650	2.870
$2\,^1S$	1	1	0.998451	1.992
	1	2	0.001185	4.812
	2	1	−0.00061	0.528
	2	2	0.001299	1.210
	1	3	−0.117763	1.992
	1	4	−0.006733	4.812
	2	3	1.176333	0.528
	2	4	−0.315588	1.210

[a] The orbital exponents are optimized in both the $1\,^1S$ and $2\,^1S$ calculations.

[b] Reference 68.

$$\Psi_2 = (1/\sqrt{2})[u(\vec{r}_1)v(\vec{r}_2) + v(\vec{r}_1)u(\vec{r}_2)]\eta(1,2) \quad , \tag{19}$$

in which

$$u(\vec{r}_k) = \sum_{n=1}^{2} \sum_{i=1}^{2} c_{ni}\, \chi_{ni}(r_k) \quad , \tag{20}$$

$$v(\vec{r}_k) = \sum_{n=1}^{2} \sum_{i=3}^{4} c_{ni}\, \chi_{ni}(r_k) \quad . \tag{21}$$

The χ_{ni} are normalized Slater atomic orbitals of principal quantum number n and orbital exponent Z_{ni}. The coefficients and orbital exponents were determined by solving the SCF equation[72] and are given in Table V. The resulting approximate energy is given in Table VI and is an upper bound to the exact $2\,^1S$ energy. To ensure reasonable values for calculated transition moments (see Sec. III C), we found it necessary to consider a $2\,^1S$ wave function which was orthogonal to our approximate $1\,^1S$ wave function. The new wave function is

$$\Psi(2\,^1S) = [1/(1-S^2)^{1/2}][\Psi_2(2\,^1S) - S\Psi_1(1\,^1S)] \quad , \tag{22}$$

where

$$S = \langle \Psi(2\,^1S) \,|\, \Psi_1(1\,^1S) \rangle = -0.014\,984\,79 \quad . \tag{23}$$

The properties of the orthogonalized SCF wave function $\Psi(2\,^1S)$ are compared in Table VI with those of several other wave functions, many of which include configuration interaction. The table shows that the orthogonalized SCF wave function gives a charge distribution for the excited state in good agreement with the accurate one of Pekeris.[73] The table also shows that the properties of the SCF wave function are not much changed by orthogonalization to the approximate $1\,^1S$ wave function.

C. Generalized Oscillator Strengths

The DCS can be written in terms of the generalized oscillator strength for all of the first-order methods discussed here. The effect on the calculated cross sections of the use of approximate wave functions has been discussed by numerous authors.[5,7,69,74]

Accurate generalized oscillator strengths for the $1\,^1S \rightarrow 2\,^1S$ transition have been calculated by Kim and Inokuti[5] using the Weiss[67] correlated wave functions, and also by Bell, Kennedy, and Kingston[75] using the same wave functions. The results of these two calculations generally agree to three significant figures. The generalized oscillator strengths obtained using the orthogonalized SCF wave functions discussed above with both the theoretical and experimental values of the excitation energy ΔE are compared in Table VII with the values tabulated by Bell *et al.*[75] Also included

TABLE VI. Energies and second moments for helium wave functions.

State	Ref.	Energy (hartrees)	$\langle r_1^2 + r_2^2 \rangle$ (a_0^2)	No. of parameters	SCF
$1\,^1S$	Hylleraas[a]	−2.8475	2.1070	1	Yes
	Clementi[b]	−2.861 67	2.3712	3	Yes
	Cohen *et al.*[c]	−2.872 51	...	6	No
	Stewart *et al.*[d]	−2.903 32	2.3872	5	No
	Weiss[e]	−2.903 72	...	54	No
	Pekeris[f]	−2.903 72	2.3870	1078	No
$2\,^1S$	Morse *et al.*[g]	−2.1475	21.7	3	No
	Marriott *et al.*[h]	−2.144 39	38.8	3	No
	Cohen *et al.*[c]	−2.143 45	...	8	No
	Present (nonorthog.)[i]	−2.143 74	33.372	10	Yes
	Present (orthog.)[j]	−2.143 74	33.419	10	No
	Coolidge *et al.*[k]	−2.144 07	33.1	13	No
	Hylleraas *et al.*[l]	−2.144 90	...	6	No
	Knox *et al.*[m]	−2.145 59	32.36	not given	No
	Weiss[e]	−2.145 97	...	55	No
	Pekeris[n]	−2.145 97	32.178	444	No

[a] E. A. Hylleraas, Z. Physik 54, 347 (1929).
[b] Reference 68.
[c] M. Cohen and R. P. McEachran, Proc. Phys. Soc. (London) 92, 37 (1967).
[d] A. L. Stewart and T. G. Webb, Proc. Phys. Soc. (London) 82, 532 (1963).
[e] Reference 67.
[f] Reference 71.
[g] P. M. Morse, L. A. Young, and E. S. Haurwitz, Phys. Rev. 48, 948 (1935).
[h] R. Marriott and M. J. Seaton, Proc. Phys. Soc. (London) A70, 296 (1957).
[i] Not orthogonal to $1\,^1S$ wave function of Ref. 68.
[j] Orthogonal to $1\,^1S$ wave function of Ref. 68.
[k] A. S. Coolidge and H. M. James, Phys. Rev. 49, 676 (1936).
[l] E. A. Hylleraas and B. Undheim, Z. Physik 65, 759 (1930).
[m] H. O. Knox and M. R. H. Rudge, J. Phys. B 2, 521 (1969).
[n] Reference 73.

TABLE VII. Generalized oscillator strengths Φ as a function of momentum transfer q in the length formation. (The numbers in parentheses are powers of 10 by which the preceding numbers are to be multiplied.) ΔE is the value of the excitation energy used for calculating cross sections with each set of oscillator strengths.

q (a.u.)	Orthog.[a]	Orthog.[a]	Nonorthog.[a]	Schneider[b]	BKK[c] (accurate)	BK[d] case A	BK[d] case B	Kennedy[e]
0.001	7.2027(−8)	6.8283(−8)	1.3609(+3)	~0				
0.01	7.4671(−6)	7.0789(−6)	1.3629(+1)					8.3622(−6)
0.10	7.3634(−4)	6.9806(−4)	1.5627(−1)		8.241(−4)	7.38(−4)	8.43(−4)	8.2406(−4)
0.20	2.8208(−3)	2.6742(−3)	5.5747(−2)	3.3588(−3)	3.154(−3)	2.83(−3)	3.22(−3)	3.1538(−3)
0.40	9.5234(−3)	9.0284(−3)	3.4955(−2)		1.061(−2)	9.53(−3)	1.08(−2)	1.0607(−2)
0.50	1.3147(−2)	1.2464(−2)	3.4198(−2)	1.5540(−2)	1.460(−2)	1.46(−2)		
0.70	1.8761(−2)	1.7786(−2)	3.4201(−2)	2.2032(−2)	2.070(−2)			
0.80	2.0276(−2)	1.9222(−2)	3.3567(−2)	2.3722(−2)	2.228(−2)	2.01(−2)	2.21(−2)	2.2276(−2)
0.90	2.0861(−2)	1.9777(−2)	3.2263(−2)	2.4314(−2)	2.282(−2)			
1.00	2.0616(−2)	1.9544(−2)	3.0346(−2)	2.3936(−2)	2.245(−2)	2.03(−2)	2.19(−2)	2.2450(−2)
1.10	1.9704(−2)	1.8680(−2)	2.7959(−2)					
1.20	1.8315(−2)	1.7363(−2)	1.5280(−2)		1.976(−2)	1.78(−2)	1.90(−2)	
1.30	1.6633(−2)	1.5768(−2)	2.2489(−2)	1.9105(−2)				
1.40	1.4816(−2)	1.4045(−2)	1.9702(−2)		1.582(−2)			
1.50	1.2987(−2)	1.2312(−2)	1.7054(−2)	1.4835(−2)				
1.60	1.1234(−2)	1.0650(−2)	1.4609(−2)	1.2806(−2)	1.188(−2)	1.05(−2)	1.11(−2)	
1.80	8.1541(−3)	7.7302(−3)	1.0463(−2)	9.3686(−3)	8.526(−3)			
2.00	5.7544(−3)	5.4553(−3)	7.3267(−3)	6.5311(−3)	5.946(−3)	5.16(−3)	5.41(−3)	
3.00	8.9353(−4)	8.4708(−4)	1.1317(−3)		8.605(−4)			
4.00	1.5533(−4)	1.4726(−4)	1.9828(−4)		1.406(−4)			
5.00	3.3034(−5)	3.1317(−5)	4.2439(−5)		2.896(−5)			
10.00					1.085(−7)			1.0849(−7)
20.00					1.791(−10)[f]			
ΔE (a.u.)	0.7576[g]	0.7182[h]	0.7576[g]		0.75775[h]	0.7599[h]	0.729[h]	0.7578[h]
$\lim_{q\to 0} \frac{\Phi(q)}{q^2}$	7.4671(−2)	7.079(−2)	1.3629(+5)		8.3616(−2)[f]	7.5(−2)	8.6(−2)	8.3261(−2)

[a]Present work.
[b]Reference 76.
[c]Reference 75.
[d]K. L. Bell and A. E. Kingston, J. Phys. B 1, 521 (1968).
[e]D. J. Kennedy, J. Phys. B 1, 526 (1968).
[f]Reference 5.
[g]Experimental value.
[h]Theoretical value.

in the table are the results obtained for the nonorthogonalized 2^1S wave function and the recent results of Schneider,[76] who calculated this quantity utilizing linear-response theory. One notes that the result obtained with the nonorthogonal 2^1S SCF wave function is extremely poor for momentum transfer $q \lesssim 1.5$, even though this wave function gives reasonably accurate energies and second moments. The result from the orthogonal SCF wave function is smaller than the accurate result of Bell *et al.*[75] for all values of $q \leq 2.4$ a.u., and the same conclusions reached in the study of the 2^1P excitation[7] concerning the reliability of SCF wave functions also apply here. On the other hand, the results obtained by Schneider[76] are larger than the accurate values for all values of q. Since a separate wave function was not calculated by Schneider in applying linear-response theory, the differences between his results and the accurate values cannot be analyzed in the same manner.

All our calculations of 2^1S DCS's and $2^1S/2^1P$ DCS ratios using the methods which include polarization were carried out using the experimental value of ΔE and SCF wave functions, i.e., Ψ_1 [Eq. (17)] for the 1^1S state, $\Psi(2^1S)$ [Eq. (22)] for the 2^1S state, and the 2^1P wave function of Eq. (33) of Ref. 7. When it is not stated otherwise, calculations of DCS's and ratios which do not include polarization are performed using the accurate $1^1S \rightarrow 2^1S$ generalized oscillator strengths.[5,75]

IV. COMPARISON OF THEORETICAL AND EXPERIMENTAL DCS's

A. Ratios

In this section we consider the ratio of the DCS for excitation of the 2^1S state to that for excitation of the 2^1P state.

1. *Energy Dependence*

At energies above 100–150 eV the Born and polarized Born approximation give similar results. The intermediate- and low-energy-ratio data exhibit two trends which are qualitatively predicted by the calculations. First, the low-angle ($\theta < 15°$)

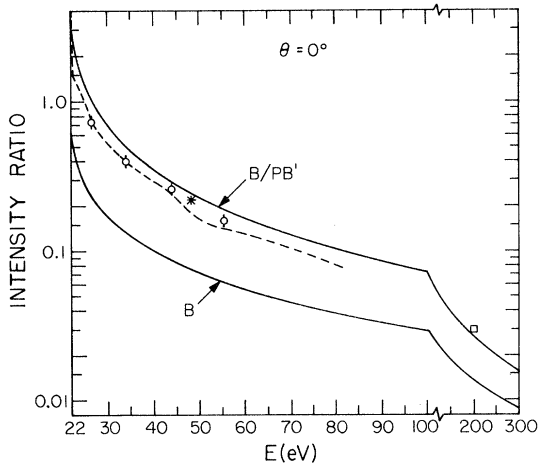

FIG. 9. $2^1S/2^1P$ intensity ratio at a scattering angle of 0° as a function of impact energy. The dashed line is the (interpolated) experimental results of Chamberlain *et al.* (Ref. 19), the circles (with error bars) are the present experimental results, the asterisk is the result of Lassettre *et al.* (Ref. 25), and the square is the result of Lassettre *et al.* (Ref. 18). The curves are calculated in the indicated approximation. $\alpha = 1.584a_0^3$ and $b = \frac{5}{4}b_1^{FW}$ at each energy. (Note the change in the impact energy scale at energies above 100 eV.)

ratios increase with decreasing impact energy (see particularly Figs. 2 and 9–11), and second, the large-angle ($\theta > 60°$) ratios increase with increasing impact energy (see particularly Figs. 2 and 12).

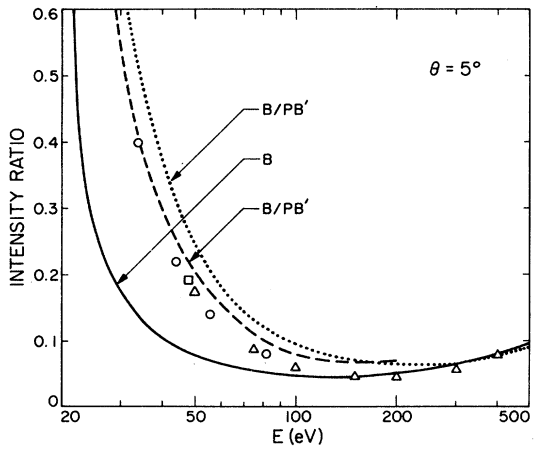

FIG. 10. $2^1S/2^1P$ intensity ratios vs energy at $\theta = 5°$. The circles are interpolated from the present experimental results, the square is an experimental value from Ref. 25, and the triangles are experimental values from Ref. 14. The curves are calculated in the Born (B) and polarized Born (B/PB′) approximations. The dotted curve is calculated with $\alpha = 1.584a_0^3$ and $b = \frac{5}{4}b_1^{FW}$ (see Sec. III A) at each energy; the dashed curve is calculated with $\alpha = 1.584a_0^3$ and with b equal to the value determined empirically (see Sec. IV A 1).

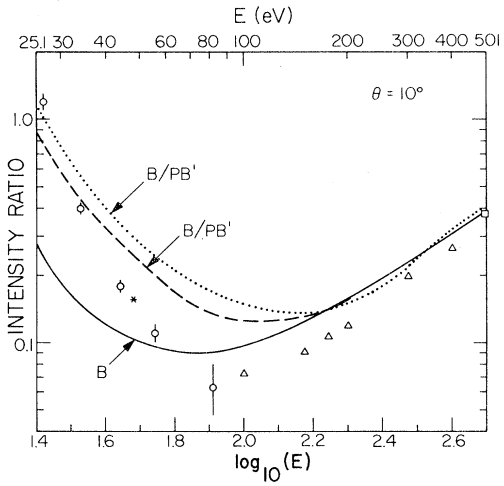

FIG. 11. $2^1S/2^1P$ intensity ratio at a scattering angle of 10° as a function of impact energy. The triangles are the experimental data of Vriens *et al.* (Ref. 2), the asterisk is the result of Lassettre *et al.* (Ref. 25), and the square is interpolated from the results of Silverman and Lassettre (Ref. 10). The curves are calculated in the approximations as indicated. The dotted curve is calculated with $\alpha = 1.584a_0^3$ and $b = \frac{5}{4}b_1^{FW}$ at each energy. The dashed curve (shown only for $E \leq 200$ eV) is calculated with $\alpha = 1.584a_0^3$ and with b equal to the value determined empirically from the $2^1S/2^1P$ ratios at 0° at each energy.

Figures 9–12 show that the theory and experiment are in better agreement for the ratios at small θ than at large θ. They also show that the theory predicts the energy dependence of the ratios better than it predicts the ratios themselves. The Born approximation (either with or without correcting for exchange) is about a factor of 3 too low for the $2^1S/2^1P$ ratios at 0°. Including polarization in the calculation of the DCS for the 2^1S state (using the theoretically most justified polarization model; see Sec. III A) gives DCS ratios at 0° and 5° in much better agreement with experiment, especially in the intermediate-energy region. This result indicates that including polarization in the description of the 2^1S excitation is necessary to describe the 2^1S and 2^1P excitation processes to the same degree of accuracy.

The 0° ratios are predicted more accurately by the first Born approximation at very high energies than at lower ones. Boersch, Geiger, and Schröder[23] obtain a $2^1S/2^1P$ intensity ratio of $(1.43 \pm 0.27) \times 10^{-4}$ at 25 keV and $\theta = 0°$. This ratio is calculated to be 1.03×10^{-4} and 1.05×10^{-4} using the Born approximation with the accurate[5,74] and orthogonalized SCF (with the experimental ΔE) oscillator strengths, respectively. The inclusion of polarization in the 2^1S state slightly improves the agreement between experiment and theory. With $\alpha = 1.584a_0^3$ and $b = \frac{5}{4} \times b_1^{FW}$, the B/PB′ approximation yields a $2^1S/2^1P$

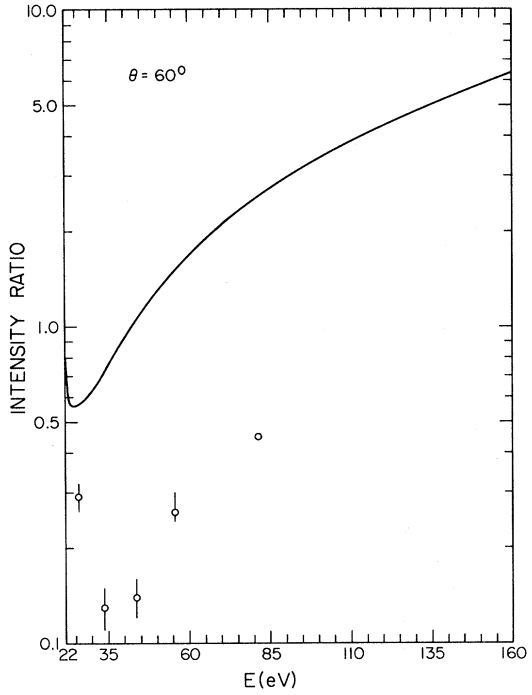

FIG. 12. Ratio of the DCS for excitation of the 2^1S state to that for excitation of the 2^1P state as a function of incident energy at $\theta = 60°$. The curve is calculated in the symmetrized Born-Ochkur-Rudge approximation (BORB I). The circles are the present experimental results. The error limits are the average deviation for 3–6 runs. No error estimate has been made for the 81.6-eV point.

ratio of 1.10×10^{-4}. Calculations using the other polarization forms give results within a few percent of this value. The polarization potential is highly nonadiabatic at this energy (note the large b_1^{FW} in Table IV), and, hence, it contributes relatively little to the scattering even at 0°.

The calculations including polarization with the theoretically justified value of b are not in exact agreement with experiment for the 0° ratio (see Fig. 10). If, however, with a fixed α we let the cutoff parameter b in the polarized Born approximation for the excitation of the 2^1S state be an empirical quantity, we can adjust it at each energy to make the calculated $2^1S/2^1P$ DCS ratio at 0° equal the experimentally measured one. The value of b determined in this manner depends on the form chosen for the polarization potential cutoff function. These results are shown in Fig. 13, which compares these empirically determined cutoff parameters to the theoretically justified b_1^{FW}. The agreement is very good. Thus, we can use the Fetter-Watson criterion to obtain a good estimate of the cutoff parameter b.

The effects of distortion of the scattering-electron wave function and exchange are small at small scattering angles. However, these effects are presumably large at 60°. Also, the short-range form of the polarization potential (i.e., the choice of polarization cutoff function in the present calculations) is much more important at $\theta = 60°$ than it is at small scattering angles. For these reasons the present calculations do not predict the cross sections accurately at scattering angles as large as 60° (see Fig. 12).

2. *Angle Dependence*

Table VIII compares the $2^1S/2^1P$ DCS ratios given by the Born approximation and three methods[7] which include exchange at several angles and two energies. The angular dependence of these predicted ratios are quite similar, particularly at higher impact energies and lower scattering angles. Thus, the form chosen for the exchange correction has only a small effect on the calculated ratios.

The present calculations are shown to be in excellent agreement with the high-energy ratio data of Silverman and Lassettre[10] at 500 eV (see Fig. 14), with that of Lassettre, Krasnow, and Silverman[9] at 511 and 417 eV (see Fig. 14), and with the experimental results of Vriens, Simpson, and Mielczarek[2] at 400 (see Fig. 15) and 300 eV (see Fig. 16). Apparently, theory and experiment[9] differ at 604 eV. The lack of high-energy experimental data for $\theta > 15°$ precludes a more rigorous test of these first-order methods for large-angle high-energy scattering. At high energies, polarization is only significant at relatively small scat-

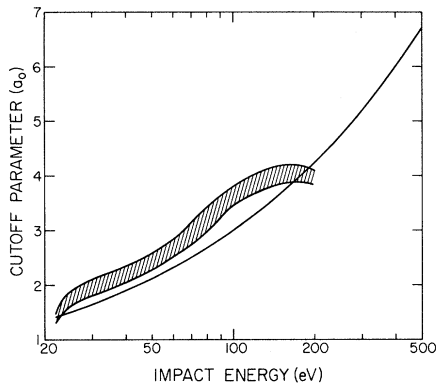

FIG. 13. Cutoff parameter (b) vs impact energy. The solid line is $b = b_1^{FW} = k_0/0.903\,72$. The shaded area encloses the range of b values determined empirically from the $2^1S/2^1P$ cross-section ratios at 0°. The empirically determined b values for the A, B, B', and C forms of the polarization potentials are scaled by multiplying them by $4/\pi$, $\frac{3}{4}$, $\frac{4}{5}$, and 1, respectively. The lowest value at each energy corresponds to the C form of the polarization potential and the highest to the A form. The scaled b values for the B, B', and C forms differ by only 1–2% at each energy.

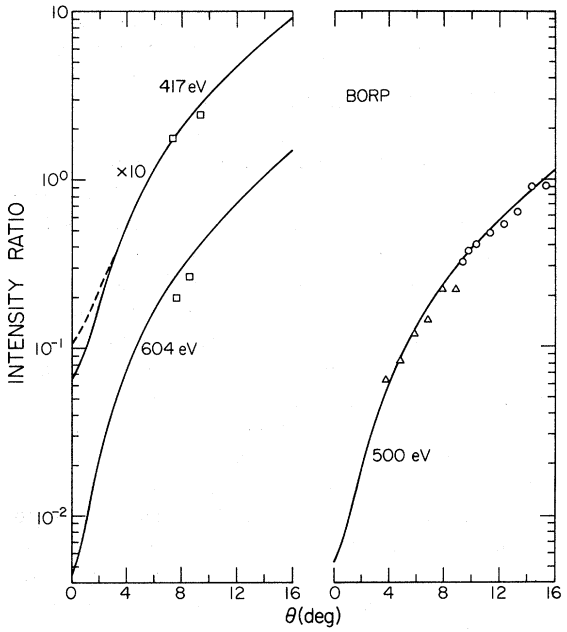

FIG. 14. $2\,^1S/2\,^1P$ intensity ratios vs scattering angle. The squares (417 and 604 eV) and triangles (511 eV) are the results of Lassettre *et al.* (Ref. 9), and the circles (500 eV) are the results of Silverman and Lassettre (Ref. 10). The dashed curve is calculated in the B/PC approximation with $\alpha = 1.584a_0^3$ and $b = b_1^{FW} = 6.13a_0$. The solid curves are calculated in the post Born-Ochkur-Rudge approximation (BORP). The results of the BORP and the first Born approximation are indistinguishable in the energy and angle range of this figure.

TABLE VIII. $2\,^1S/2\,^1P$ DCS ratios calculated in the Born (B), prior Born-Ochkur-Rudge (BOR), post Born-Ochkur-Rudge (BORP), and Born-transferred Kang-Foland (BTKF) approximations.

Scattering angle (deg)	Method B	BOR	BORP	BTKF
		$E = 30$ eV		
0	0.170	0.168	0.173	0.169
30	0.289	0.285	0.297	0.288
60	0.620	0.609	0.650	0.617
90	1.18	1.16	1.29	1.16
120	1.81	1.78	2.08	1.77
150	2.27	2.24	2.66	2.24
180	2.44	2.41	2.86	2.42
		$E = 300$ eV		
0	0.00898	0.00898	0.00898	0.00898
30	2.83	2.83	2.84	2.84
60	17.5	17.5	17.7	17.5
90	52.2	52.1	61.4	52.7
120	92.8	92.4	96.6	94.7
150	124	123	126	126
180	135	135	137	137

tering angles. The data presently available do not cover the low-angle region well enough to allow a definitive test of the importance of polarization at these energies.

As the impact energy is lowered to 225 eV and below, the ratios calculated either with or without polarization increase more rapidly with increasing angle than do the experimental ones (see Fig. 16). However, even at impact energies as low as 81.6 eV (see Fig. 3), the calculated ratios are within about a factor of 5 of the experimental ones to angles as large as 80° and exhibit a variation with angle which is qualitatively correct. At energies below 81.6 eV, the ratios calculated without polarization differ markedly in both magnitude and shape from the experimental ones (see Figs. 1 and 2). However, Figs. 9–11 show that the inclusion of polarization in the calculation significantly improves

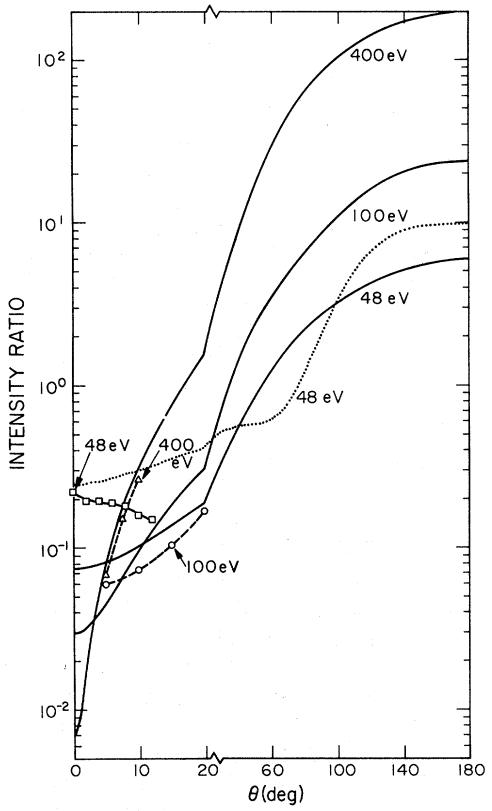

FIG. 15. $2\,^1S/2\,^1P$ intensity ratios. The triangles and circles are the experimental results of Vriens *et al.* (Ref. 2) at 400 and 100 eV, respectively. The squares are the experimental results of Lassettre *et al.* (Ref. 25) at 48 eV. The solid curves are calculated in the Born-transferred Kang-Foland (BTKF) approximation at the indicated energy. The dotted curve is calculated at 48 eV in the B/PB′ approximation with $\alpha = 1.584a_0^3$ and b empirically determined to be $2.08a_0$. A curve for the Born approximation at 400 eV would be indistinguishable from the BTKF curve on the scale of this figure.

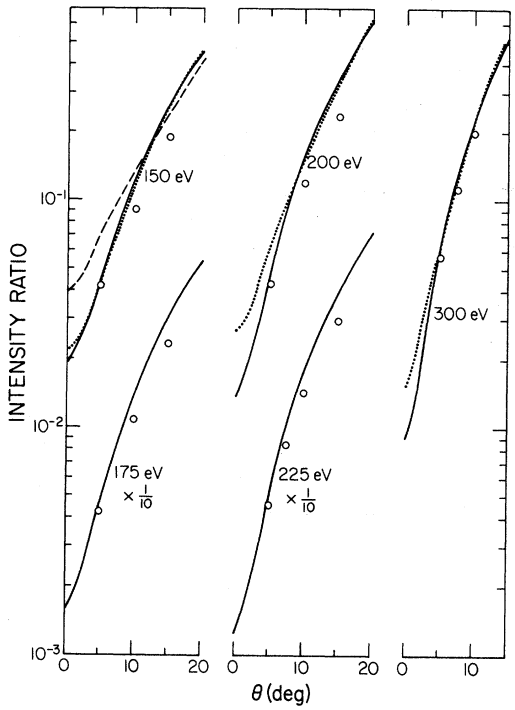

FIG. 16. $2\,^1S/2\,^1P$ intensity ratios as a function of scattering angle at the indicated energies. The circles are the experimental results of Vriens *et al.* (Ref. 2). The solid curves are calculated in the BTKF approximation. The dashed and dotted curves are calculated in the B/PB′ approximation with $\alpha = 1.584a_0^3$, $b = \frac{5}{4}b_1^{FW} = 4.59a_0$ for the dashed curve, $b = 2(\frac{5}{4})b_1^{FW} = 9.18a_0$ for the dotted curve at 150 eV; $b = \frac{5}{4}b_1^{FW} = 5.30a_0$ for the dotted curve at 200 eV; and $b = \frac{5}{4}b_1^{FW} = 6.50a_0$ for the dotted curve at 300 eV.

the agreement between theory and experiment at small angles.

B. DCS Angle Dependence

The experimental and calculated DCS's for the 0°–90° angular range are shown in Figs. 4–8 for several energies below 100 eV (26.5, 34, 44, 55.5, and 81.6 eV) and in Fig. 17 for the 0°–20° range at several higher energies (100, 150, 175, 200, 225, 300, and 400 eV). Although the Ochkur and the symmetrized Born-Ochkur-Rudge DCS's have zeros at some scattering angles, the different first-order calculations predict approximately the same angular behavior, which can be simply characterized in most of the cases as monotonically decreasing as the scattering angle increases and becoming steeper as the impact energy increases. The agreement between the theoretical and the available experimental results becomes much better at impact energies of 81.6 eV and above.

The comparison of theory and experiment is most interesting in the small-angle region where the effects of distortion and exchange are minimum.

Previous work on the effect of polarization for elastic scattering showed that polarization is especially important for small-angle scattering.[8,40,41,63–65,77] In the present case of inelastic scattering, the best agreement between the experimental and theoretical angular dependence at small angles is obtained for the B/PB′ calculations as shown on Figs. 5–7. These curves are easily seen to be much steeper than the Born (B) curve. Unfortunately, at very small angles the magnitudes of these curves deviate the most from the experimental values. (For ease of comparison of their angular dependence with experiment, these curves were renormalized to the experimental DCS's at 10° by multiplying the calculated values by a factor of 0.281, 0.230, and 0.193 for the energies of 34, 44, and 55.5 eV, respectively.)

The plane-wave theories used here overestimate the magnitude of the DCS as they did for excitation of the $2\,^1P$ state.[7] However, in that case we found that the Born approximation and the Ochkur-like approximations gave approximately the correct angle dependence of the DCS for momentum transfers less than about 1.6 a.u. This corresponds to about 40° in the intermediate-energy range. Figures 4–7, however, show that the Born approximation and the Ochkur-like approximations (neglecting polarization) do not predict the correct angular dependence for excitation of the $2\,^1S$ state

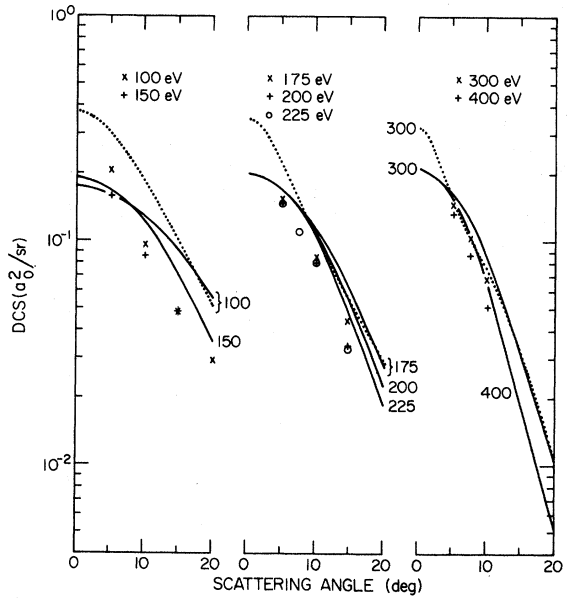

FIG. 17. $2\,^1S$ DCS. The solid curves are the DCS calculated in the post Born-Ochkur-Rudge approximation (BORP) and the symbols represent the data of Ref. 2. The impact energies in eV are indicated next to the curves and symbols. The dotted curves are calculated in the polarized Born approximation (B/PB′) with $\alpha = 1.584a_0^3$ and $b = \frac{5}{4}b_1^{FW}$ at each energy.

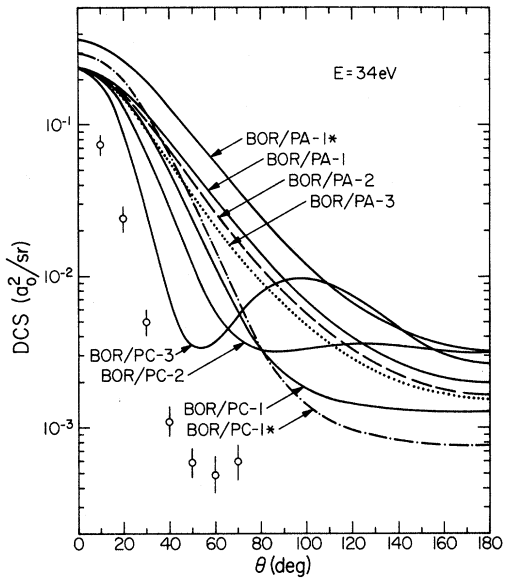

FIG. 18. 2^1S DCS at $E=34$ eV calculated in the polarized Born-Ochkur-Rudge approximation (BOR/P) with form A and form C polarization potentials. The numbers 1, 2, and 3 after the designations refer to $\alpha=1.584a_0^3$, $\alpha=3.0a_0^3$, and $\alpha=7.0a_0^3$, respectively. The cutoff parameter used in the polarization potential is b_l^{FW} for the BOR/PC-1* and $\frac{1}{4}\pi\, b_l^{FW}$ for the BOR/PA-1* curves, and is determined empirically (see text) for the others. The circles with error bars represent the present data.

even at angles considerably less than 40°. The inclusion of polarization, making the adiabatic approximation in the initial state, brings theory and experiment into better qualitative agreement for the angle dependence. In the Appendix, we discuss more fully the angle range over which plane-wave theories agree with experiment for the helium 2^1P and 2^1S excitations as well as for elastic scattering by He, Hg, and H_2.

The effect of the choice of polarization potential on the DCS's is explicitly shown in Figs. 18 and 19 for $E=34$ and 81.6 eV, respectively. The calculations shown in these figures were carried out in the BOR/P approximation with different types of cutoff functions and with different values of α and b. At lower impact energies (e.g., 34 eV) we can draw the following general conclusions: In the BOR/PA calculations the angle dependence of the DCS's are not affected appreciably by changes in either α or b. In the BOR/PC calculations, as the value of α is increased the DCS curves become steeper at low angles and a minimum and a maximum develop in the curve at intermediate angles. These minima and maxima shift to lower angles as α is increased. The behavior of the DCS's calculated in the BOR/PB and BOR/PB′ approximations is intermediate between those of the BOR/PA and BOR/PC approximations.

Attempts at determining the transition polarizability empirically from the present data indicate that it cannot be determined with any accuracy. The best agreement with experiment at 34 eV is obtained with polarization form C and with $\alpha\approx 7a_0^3$. This value of α is considerably larger than the theoretically justified value of $1.584a_0^3$. However, the value of α required for the best agreement with experiment decreases with increasing energy in contrast to the energy independence of this quantity when it is determined theoretically. At higher impact energies (81.6 eV) all the calculated curves fall into a relatively narrow band, and they predict the magnitude of the DCS's in agreement with experiment out to about 70°. The calculations are not expected to be reliable at large scattering angles because of uncertainties in the proper short-range form of the polarization potential. At energies near 100 eV and higher the influence of α and b is significant only at small scattering angles, where the lack of experimental data precludes a definitive test of these calculations.

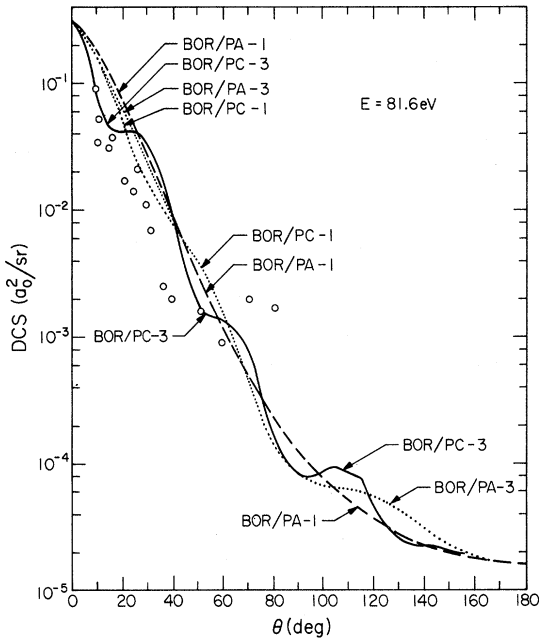

FIG. 19. 2^1S DCS's at 81.6 eV calculated in the polarized Born-Ochkur-Rudge approximation (BOR/P) with form A and form C polarization potentials. The numbers 1 and 3 after the symbols refer to $\alpha=1.584a_0^3$ and $\alpha=7.0a_0^3$, respectively. The cutoff parameter used in the polarization potential is determined from the experimental $2^1S/2^1P$ intensity ratios at $\theta=0°$ (see text).. The BOR/PA-3 curve is shown only up to $\theta=40°$ because at higher angles it cannot be distinguished from the BOR/PA-1 curve on the scale of this figure. Curves for BOR/PA and BOR/PC with $\alpha=3.0a_0^3$ are not shown since they are intermediate between the two cases shown. The circles are the present data.

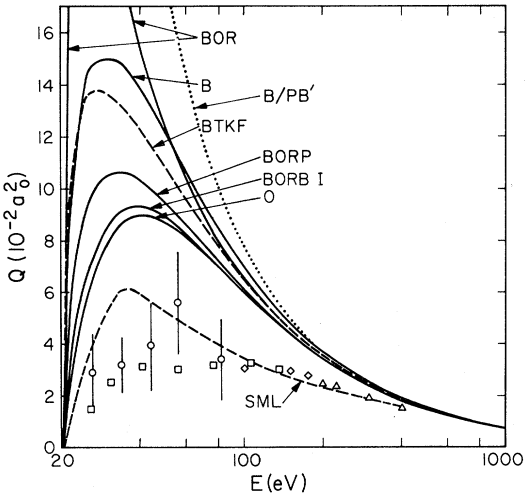

FIG. 20. $1\,^1S \rightarrow 2\,^1S$ integral cross sections as a function of impact energy. The squares are the experimental results of Dugan *et al.* (Ref. 27) (corrected for cascade, see text); the triangles and diamonds are those of Vriens *et al.* (see text) (Ref. 2); and the circles (with error bars) are the present experimental results (see text). The curve labeled SML is obtained by scaling the $3\,^1S$ excitation function data of St. John, Miller, and Lin (Ref. 79) (see text). The other curves are calculated using the indicated approximations. For the polarized Born approximation (B/PB'), $\alpha = 1.584a_0^3$ and $b = \frac{5}{4}b_1^{FW}$ at each energy. The low energy rise in the B/PB' cross section (not shown) is steeper than that of the Born-Ochkur-Rudge approximation (BOR).

It is interesting to consider using the final-state polarization interaction with the very large values of the cutoff parameter suggested by the Fetter-Watson criterion (see Table IV). Although α_{21} is much larger than α_{12}, b_2^{FW} is so large that adding this interaction does not even change the first few significant figures of the calculated DCS.

V. COMPARISON OF THEORETICAL AND EXPERIMENTAL INTEGRAL CROSS SECTIONS

The integration of our experimental $2\,^1S$ DCS's to obtain $2\,^1S$ integral cross sections is discussed in Sec. II, and the results are plotted in Fig. 20. The high-energy (200, 225, 300, and 400 eV) experimental integral cross sections obtained by Vriens, Simpson, and Mielczarek[2] are shown in this figure. The cross sections at 100, 150, and 175 eV were obtained by integrating the $2\,^1S$ DCS fits given by these authors. These latter results are subject to some uncertainty since only a small range of angles ($\theta \leq 20°$) was studied. We obtained the remaining experimental cross sections in Fig. 20 by an analysis of the excitation-function measurements of Dugan, Richards, and Muschlitz[27] as discussed below.

Dugan, Richards, and Muschlitz[27] measured the relative electron-impact excitation function $R(E)$ for production of the $2\,^1S$ state for $26 \leq E \leq 136$ eV. Their excitation function includes contributions from radiative decay to the $2\,^1S$ state by higher states (cascade) excited by electron impact, i.e.,

$$Q(E) \cong \lambda R(E) - \sum_{n=2} Q_n(E) A(n\,^1P - 2\,^1S) \ , \qquad (24)$$

where the last term is the cascade correction, λ is independent of E and normalizes their relative data to the absolute scale, $Q_n(E)$ is the integral cross section for excitation of the $n\,^1P$ state, A is the branching fraction for $n\,^1P \rightarrow 2\,^1S$ radiative decay, and $Q(E)$ is the $2\,^1S$ integral cross section. The branching fractions for $n = 2$–8 are calculated from the table given by Gabriel and Heddle.[78] Since the $3\,^1P$ state is the largest contributor to the cascade correction, we use the n^3 rule to express the other ^1P cross sections in terms of the $3\,^1P$ cross section, i.e.,

$$Q_n(E) = (3/n)^3 Q_3(E), \quad n = 2, 4, 5, \ldots \ . \qquad (25)$$

We then obtain

$$Q(E) \cong \lambda R(E) - 0.0527 Q_3(E) \ . \qquad (26)$$

We use the absolute values of $Q_3(E)$ of St. John, Miller, and Lin (SML).[79] The value of λ in Eq. (26) is determined by requiring that $Q(136\text{ eV}) = 0.030a_0^2$, which is chosen to be in reasonable agreement with the lower energy data of Vriens, Simpson, and Mielczarek.[2] The resulting cross section values $Q(E)$ are plotted in Fig. 20.

The curve in Fig. 20 labeled SML is obtained by assuming that the shape of the $2\,^1S$ integral cross section curve is the same as the $3\,^1S$ one measured by SML[79] as a function of the incident energy in threshold units $[E/\Delta E(1\,^1S - n\,^1S)]$. The ordinate for this curve is determined by normalizing it to the $E = 300$-eV integral cross-section data of Vriens, Simpson, and Mielczarek.[2]

The different measurements for the $2\,^1S$ integral cross section shown in Fig. 20 are in good accord with each other with the possible exception of the result deduced from the SML data below about 50 eV.

The other curves in Fig. 20 represent the various theoretical models discussed in Sec. III, both with and without polarization as indicated. The total cross sections calculated with the BOR and B/PB' ($\alpha = 1.584a_0^3$) models reach maxima of about $0.21 \times a_0^2$ and $0.37a_0^2$, respectively, within 1 eV of 26 eV. Figure 21 presents some additional integral cross sections calculated using several forms of the polarization potential. This figure shows the sensitivity of the magnitudes of the B/P cross sections to the form of the short-range part of the polarization potential.

The cross sections predicted by the first-order

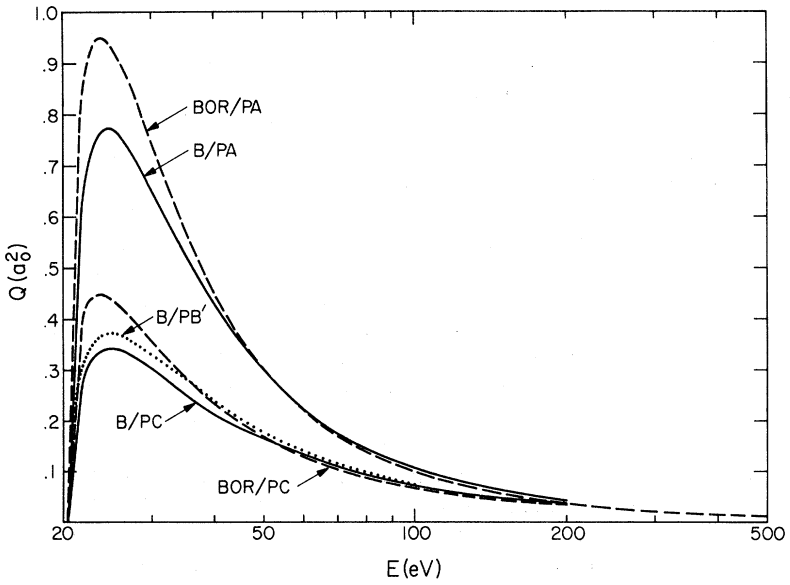

FIG. 21. $2\,^1S$ integral cross sections calculated in the indicated approximation including polarization. $\alpha = 1.584 a_0^3$ for all curves. $b = b_1^{FW}$ for polarization potential form C, $b = \frac{5}{4} b_1^{FW}$ for form B', and $b = \frac{1}{4\pi} b_1^{FW}$ for form A at each energy.

theories apparently agree well with experiment for energies greater than about 400 eV but are too large for lower energies. Lassettre[80] used the Born approximation and a generalized oscillator strength fitting procedure to obtain the $2\,^1S$ integral cross section at all energies based on experimental generalized oscillator strengths measured only at high energies. His cross-section curve lies very close to the Born-transferred Kang-Foland (BTKF) curve in Fig. 20 and somewhat below the Born approximation results based on the accurate generalized oscillator strengths of Kim and Inokuti.[5] Schneider[76] used a generalized oscillator strength calculated using linear-response theory to calculate an integral cross section at 500 eV. His value is just slightly (10%) larger than that given by the pure Born result using the orthogonalized SCF wave functions. As in the case of the $2\,^1P$ excitation,[7] the Ochkur (O) and symmetrized Born-Ochkur-Rudge (BORB I) approximations give considerable improvement over the Born approximation in the shape of the cross section, although they still overestimate it. The inclusion of polarization with a given first-order theory results in an even larger integral cross section.

VI. SUMMARY AND CONCLUSION

Experimental and quantum-mechanical results are presented for the integral and differential cross sections for excitation of the $2\,^1S$ state and for the ratio of DCS's for excitation of the $2\,^1S$ and $2\,^1P$ states in the impact energy range 26.5–81.6 eV. Calculations based on seven first-order theories which do not include polarization are presented: the Born (B), the prior form of the Ochkur (O), the prior form of the Born-Ochkur-Rudge (BOR), the post form of the Born-Ochkur-Rudge (BORP), the symmetrized Born-Ochkur-Rudge (BORB I), the Born-transferred Kang-Foland (BTKF), and the Born-transferred Vainshtein-Presnyakov-Sobelman (BTVPS) approximations. Scattering by several forms of a polarization potential is combined with scattering in the Born and Born-Ochkur-Rudge approximations to yield the polarized Born (B/P) and polarized Born-Ochkur-Rudge (BOR/P) approximations. Calculations using these two approximations are presented for excitation of the $2\,^1S$ state. To explain the angle dependence of the small-scattering-angle ($\theta \lesssim 40°$) DCS for $E = 34$–81.6 eV for either transition, it is unnecessary to include an accurate treatment of the distortion of the scattering-electron wave function or of exchange of the incident electron with the bound electrons. This property of the scattering is accurately predicted using plane-wave scattering functions and an effective potential (optical potential) to represent the interaction of the scattering electron with the target. For the $2\,^1P$ excitation, the potential may be determined in the static approximation (unperturbed initial and final state) but for the $2\,^1S$ excitation it is necessary to include the induced dipole in the description of the target. Although the adiabatic polarization model was previously shown to be an adequate way to include the effect of the induced dipole on elastic scattering at impact energies at least up to a few hundred eV, this model is not adequate for the $1\,^1S \rightarrow 2\,^1S$ transition. Evidently, nonadiabatic effects are more important for inelastic scattering than for elastic scattering. We use Fetter and Watson's theoretical criterion for the applicability of the adiabatic approximation to evaluate a cutoff param-

eter for including some nonadiabatic effects in the polarization model. This procedure gives results in better agreement with experiment than those obtained by including only the static interaction, especially in the 44–81.6-eV energy range.

The present calculations agree better with higher energy ($E \gtrsim 100$ eV) experimental DCS data than do previous theoretical treatments (the first Born approximation).

We find that the calculated magnitudes of the DCS's are in poor agreement with experiment in intermediate energies. The agreement is worse in the present case than in the case of the $2\,^1P$ excitation.[7]

The usefulness of SCF single-configuration wave functions for describing the target is examined. We find, on comparing the results to those from more accurate calculations, that orthogonalized SCF wave functions reproduce many facets of the more accurate calculations with good accuracy.

The criteria developed here for the importance of polarization can be used to discuss in a consistent way the DCS's for elastic scattering of electrons by He and H_2 and for excitation of the $2\,^1S$ and $2\,^1P$ states of He.[81]

Many more details of the theoretical work and the comparison of theory and experiment are included in an extended version of this article.[82]

ACKNOWLEDGMENTS

We are grateful to Professor Aron Kuppermann and Dr. Walter Williams for their contributions to the experimental work at 26.5–55.5 eV and 81.6 eV, respectively. We are grateful to Dr. Gordon W. F. Drake of the University of Windsor for performing and sending his unpublished calculations mentioned in the text. Some of the work reported here was initiated while one of the authors (D. C. C.) was associated with the Institute for Extraterrestrial Physics of the Max Planck Institute for Physics and Astrophysics in Munich, Germany, and with the Department of Physics of the University of Colorado in Boulder, Colo., and while two of the authors (J. K. R. and D. G. T.) were associated with the Department of Chemistry of the California Institute of Technology.

APPENDIX: ANGLE RANGE OVER WHICH PLANE-WAVE THEORIES AGREE WITH EXPERIMENT

Both Rice and co-workers[83–85] and Miller, Mielczarek, and Krauss[86] have attempted to use the experimentally measured angle dependence of the DCS as an indicator of the state symmetries involved in a transition which produces a particular energy-loss peak.

The method used by Rice and co-workers is empirically based on the comparison of measured DCS ratios as a function of angle for various types of transitions.[87] However, Miller *et al.*[86] attempt to match the angle dependence of the experimental DCS to that of a Born-approximation calculation. They argue that a dip in the experimental DCS means the transition is of the type for which the Born-approximation DCS has a dip. If such reasoning is to be used confidently, we must be reasonably certain that the Born approximation predicts the correct angle dependence of the DCS in certain situations. Further, in order to decide whether plane-wave calculations for different types of transitions can be useful in guiding the method of Rice and co-workers, we must determine the range of angles for which plane-wave calculations predict the correct angle dependence of the DCS.

Table IX summarizes some of the presently available data on the range over which the Born and polarized Born approximations predict the approximately correct angle dependence of the DCS. The first three columns list the target, transition, and impact energy, respectively. The fourth column contains the maximum angle θ_{max} for which plane-wave theory and experiment have approximately the same shape. This angle is determined by normalizing theory to experiment at $\theta = 20°$ and finding the angle at which they deviate by 50%. The fifth, sixth, and seventh columns contain, respectively, the momentum transfer $q(\theta_{max})$, the experimental DCS $I^{expt}(\theta_{max})$, and the calculated DCS $I^{calc}(\theta_{max})$ evaluated at $\theta = \theta_{max}$.

The plane-wave cross sections agree qualitatively with experiment at small θ, where many partial waves contribute appreciably to the DCS. At large θ the scattering is due mainly to the lowest few partial waves where distortion of the plane wave may be appreciable.[8] To obtain a rough estimate of the contribution to scattering involving large distortion, we present in the eighth column one-half the maximum theoretical cross section for s-wave scattering I^S. (The s-wave limit for the DCS is $1/k^2$ for elastic scattering and $1/4k^2$ for inelastic scattering.[88]) Finally, the ninth and tenth columns list, respectively, the experimental and calculated DCS's divided by $\frac{1}{2} I^S$.

In a previous paper[7] we noted that for excitation of the $2\,^1P$ state, the angle dependence of the DCS was predicted out to $q \approx 1.6$ a.u. The more extensive collection of data presented in Table IX shows that for elastic scattering the plane-wave theories often predict the angle dependence correctly out to even large q. The data also indicate a systematic trend in which the angle dependence of the DCS is correctly predicted out to larger q at higher energies than at lower ones. Further, the magnitudes of the experimental and theoretical DCS's agree better at higher energy. In discussing scattering from a central potential of finite range,

TABLE IX. Range of angles over which plane-wave theories predict approximately the correct angle dependence of the DCS for elastic and inelastic scattering. The column headings are defined in the Appendix. The theoretical cross sections for elastic scattering and excitation of the He $2\,^1S$ state are calculated in the polarized Born approximation. Those for excitation of the $2\,^1P$ state of helium are calculated in the Born approximation. In cases where the theory and experiment still satisfy our criterion for agreement at the largest angle for which experimental data are available, we can only obtain lower bounds on the fourth and fifth columns and upper bounds on the sixth and seventh, and ninth and tenth columns.

Target	Transition	E (eV)	θ_{max} (deg)	q_{max} (a.u.)	I^{expt} (a_0^2/sr)	I^{calc} (a_0^2/sr)	$\frac{1}{2}I^S$ (a_0^2/sr)	$2I^{expt}/I^S$	$2I^{calc}/I^S$
He	elastic	39[a]	≥80	≥2.18	≤0.23	≤0.23	0.174	≤1.3	≤1.3
		81.6[a]	50	2.07	0.18	0.27	0.084	2.1	3.2
		500[b]	≥60	≥6.06	≤0.011	≤0.011	0.014	≤0.78	≤0.78
He	$1\,^1S \rightarrow 2\,^1S$	34	22[c]	0.76	0.020	0.18	0.050	0.40	3.6
		44	26[c]	0.85	0.007	0.11	0.039	0.18	2.8
		55.5	42	1.36	0.0016	0.013	0.031	0.052	0.42
		81.6	45	1.77	0.002	0.0052	0.022	0.091	0.24
		100[d]	≥20	≥0.94	≤0.029	≤0.051	0.017	≤1.7	≤3.0
		175[d]	≥15	≥0.93	≤0.044	≤0.055	0.0097	≤4.5	≤5.7
		300[d]	≥10	≥0.82	≤0.069	≤0.074	0.0057	≤12	≤13
		400[d]	≥10	≥0.95	≤0.052	≤0.061	0.0042	≤12	≤14
He	$1\,^1S \rightarrow 2\,^1P$	34[e]	40	1.04	0.017	0.084	0.050	0.34	1.7
		44[e]	58	1.56	0.0072	0.010	0.039	0.18	0.26
		55.5[e]	45	1.44	0.014	0.019	0.031	0.45	0.61
		81.6[e]	49	1.91	0.0067	0.0027	0.022	0.30	0.12
		100[f]	≥20	≥0.94	≤0.18	≤0.20	0.017	≤11	≤12
		175[f]	≥15	≥0.94	≤0.19	≤0.22	0.0097	≤20	≤23
		300[f]	≥10	≥0.82	≤0.35	≤0.37	0.0057	≤61	≤65
		400[f]	≥10	≥0.95	≤0.20	≤0.21	0.0042	≤48	≤50
Hg	elastic	300[g]		≥1.61	≤7.5	≤33[h]	0.028	≤268	
		400[g]		≥1.86	≤4.7	≤20[h]	0.017	≤276	
		500[g]		≥2.1	≤3.3	≤12[h]	0.014	≤236	
H_2	elastic[i]	7	115	1.21	2.0	1.3	0.97	2.1	1.3
		10	120	1.48	1.0	0.65	0.68	1.5	0.96
		13.6	≥80	≥1.29	≤1.2	≤1.2	0.50	≤2.4	≤2.4
		20	100	1.86	0.5	0.30	0.34	1.5	0.88
		45	≥80	≥2.34	≤0.15	≤0.12	0.15	≤1.0	≤0.80
		60	120	3.64	0.043	0.03	0.11	0.39	0.27
		81.6	≥80	≥3.15	≤0.058	≤0.05	0.084	≤0.69	≤0.60
		30	100	2.28		0.14	0.23		0.61
		50	110	3.14		0.05	0.14		0.36
		100	105	4.30		0.018	0.068		0.26

[a]Reference 81.

[b]J. P. Bromberg, J. Chem. Phys. 50, 3906 (1969).

[c]These angles, obtained by interpolation, are so close to 20° that they imply there is very little quantitative agreement in the angle dependence of theory and experiment.

[d]Experimental data of Ref. 2 and polarized Born-approximation calculations of present work.

[e]Reference 7.

[f]Experimental data of Ref. 2 and Born-approximation results of Ref. 7.

[g]J. P. Bromberg, J. Chem. Phys. 51, 4117 (1969).

[h]These values are $(36.5/18.65)^2$ times greater than the values in footnote g, due to an error in that calculation.

[i]Reference 65.

Schiff[89] suggests that the Born approximation can be used at all angles provided the incident energy is high enough while at lower energies the small-angle scattering may be given correctly when the large-angle scattering is not. Such a trend is consistent with the present results.

The entries in the ninth column of Table IX are near unity for the elastic scattering data and possibly the $1\,^1S \rightarrow 2\,^1P$ DCS's. This indicates that s-wave scattering may account for the values of θ_{max} obtained in these cases. However, the angle dependence of the $1\,^1S \rightarrow 2\,^1S$ DCS's is predicted to angles at which the cross section is considerably lower than our estimate of the maximum probable s-wave contribution. Possibly our use of $\frac{1}{2}I^S$ for this estimate is not as realistic in this case. In

general, the ninth column provides a less-energy-dependent criterion for the validity of the plane-wave theories than do either the fourth or fifth column.

Table IX shows that plane-wave theories are more successful for elastic scattering than for inelastic scattering. This success is probably due to the larger contributions to the cross sections from higher partial waves in the elastic case. For the two inelastic transitions in the table, the Born approximation is less valid for the 2^1S excitation than for the 2^1P one. This is probably due to the much greater difficulties in estimating the effective potential for the 2^1S case. This points up the importance of further study of the non-adiabatic-transition polarization potential.

---

*Research supported in part by the U.S. Atomic Energy Commission, by the Department of Chemistry of the University of Minnesota, by the U.S. Air Force Space and Missile Systems Organization (SAMSO) under Contract No. FO-4701-70-C-0059, and by the National Aeronautics and Space Administration under Contract No. NAS7-100.

[1]E. N. Lassettre and E. A. Jones, J. Chem. Phys. 40, 1222 (1964).

[2]L. Vriens, J. A. Simpson, and S. R. Mielczarek, Phys. Rev. 165, 7 (1968).

[3]N. F. Mott and H. S. W. Massey, *The Theory of Atomic Collisions*, 3rd ed. (Clarendon, Oxford, 1965), pp. 484–488, 499, and references therein.

[4]H. S. W. Massey and E. H. S. Burhop, *Electronic and Ionic Impact Phenomena*, 2nd ed. (Clarendon, Oxford, 1969), Vol. I, pp. 480–496.

[5]Y.-K. Kim and M. Inokuti, Phys. Rev. 175, 176 (1968).

[6]A. Skerbele and E. N. Lassettre, J. Chem. Phys. 53, 3806 (1970).

[7]D. G. Truhlar, J. K. Rice, A. Kuppermann, S. Trajmar, and D. C. Cartwright, Phys. Rev. A 1, 778 (1970). The normalization of the experimental absolute 2^1P DCS's presented there should be modified as discussed in Sec. II of this paper.

[8]D. G. Truhlar and J. K. Rice, J. Chem. Phys. 52, 4480 (1970).

[9]E. N. Lassettre, M. E. Krasnow, and S. M. Silverman, J. Chem. Phys. 40, 1242 (1964).

[10]S. M. Silverman and E. N. Lassettre, J. Chem. Phys. 40, 1265 (1964).

[11]A. Skerbele and E. N. Lassettre, J. Chem. Phys. 45, 1077 (1966).

[12]J. A. Simpson, M. G. Menendez, and S. R. Mielczarek, Phys. Rev. 150, 76 (1966).

[13]D. Andrick, H. Ehrhardt, and M. Eyb, Z. Physik 214, 388 (1968).

[14]G. E. Chamberlain, S. R. Mielczarek, and C. E. Kuyatt, Phys. Rev. A 2, 1905 (1970).

[15]G. E. Chamberlain, J. A. Simpson, S. R. Mielczarek, and C. E. Kuyatt, J. Chem. Phys. 47, 4266 (1967).

[16]J. A. Simpson and S. R. Mielczarek, J. Chem. Phys. 39, 1606 (1963).

[17]E. N. Lassettre, A. S. Berman, S. M. Silverman, and M. E. Krasnow, J. Chem, Phys. 40, 1232 (1964).

[18]E. N. Lassettre, V. D. Meyer, and M. S. Longmire, J. Chem. Phys. 41, 2952 (1964).

[19]G. E. Chamberlain, H. G. M. Heideman, J. A. Simpson, and C. E. Kuyatt, in *Abstracts of Papers of the Fourth International Conference on the Physics of Electronic and Atomic Collisions* (Science Bookcrafters, Hastings-on-Hudson, N.Y., 1965), p. 378.

[20]J. P. Doering, J. Chem. Phys. 45, 1065 (1966).

[21]J. P. Doering and A. J. Williams, J. Chem. Phys. 47, 4180 (1967).

[22]J. P. Doering (private communication).

[23]H. Boersch, J. Geiger, and B. Schröder, in *Abstracts of Papers of the Fifth International Conference on the Physics of Electronic and Atomic Collisions* (Nauka, Leningrad, 1967), p. 481.

[24]A. Skerbele and E. N. Lassettre, in Ref. 23, p. 495.

[25]E. N. Lassettre, A. Skerbele, M. A. Dillon, and K. J. Ross, J. Chem. Phys. 48, 5066 (1968).

[26]R. I. Hall, G. Joyez, J. Mazeau, and J. Reinhardt. Compt. Rend. 272, 743 (1971).

[27]J. L. G. Dugan, H. L. Richards, and E. E. Muschlitz, J. Chem. Phys. 46, 346 (1967).

[28]B. L. Moiseiwitsch and S. J. Smith, Rev. Mod. Phys. 40, 238 (1968).

[29]V. I. Ochkur, Zh. Eksperim. i Teor. Fiz. 45, 734 (1963) [Sov. Phys. JETP 18, 503 (1964)].

[30]M. R. H. Rudge, Proc. Phys. Soc. (London) 85, 607 (1965).

[31]O. Bely, Proc. Phys. Soc. (London) 87, 1010 (1966).

[32]D. S. F. Crothers, Proc. Phys. Soc. (London) 87, 1003 (1966).

[33]L. Presnyakov, I. Sobelman, and L. Vainshtein, in *Atomic Collision Processes*, edited by M. R. C. McDowell (North-Holland, Amsterdam, 1964), p. 243.

[34]I.-J. Kang and W. D. Foland, Phys. Rev. 164, 122 (1967).

[35]R. A. Bonham, J. Chem. Phys. 36, 3260 (1962).

[36]D. G. Truhlar, D. C. Cartwright, and A. Kuppermann, Phys. Rev. 175, 113 (1968).

[37]D. G. Truhlar and A. Kuppermann, in *Abstracts of Papers of the Sixth International Conference on the Physics of Electronic and Atomic Collisions*, edited by I. Andur (MIT, Cambridge, Mass., 1969), p. 247.

[38]B. L. Scott, Phys. Rev. 140, A699 (1965).

[39]Reference 3, pp. 420–422, 456–457, 480–484.

[40]Reference 4, Chap. XVIII.

[41]B. H. Bransden, *Atomic Collision Theory* (Benjamin, New York, 1970), p. 235.

[42]P. G. Burke, J. W. Cooper, and S. Ormonde, Phys. Rev. 183, 245 (1969); P. G. Burke, A. Hibbert, and W. D. Robb, J. Phys. B 4, 153 (1971).

[43]See H. C. Volkin, Phys. Rev. 155, 1177 (1965), and references therein.

[44]J. R. Oppenheimer, Phys. Rev. 32, 361 (1928).

[45]See, e.g., M. J. Seaton, Proc. Phys. Soc. (London) 77, 174 (1961).

[46]L. Castillejo, I. C. Percival, and M. J. Seaton, Proc. Roy. Soc. (London) 254, 259 (1960).

[47]M. H. Mittleman and J. L. Peacher, Phys. Rev. 173, 160 (1968).

[48]C. J. Kleinman, Y. Hahn, and L. Spruch, Phys. Rev. 165, 53 (1968).

[49]R. T. Pu, University of California Lawrence Radiation Laboratory Technical Report No. UCRL-10878, 1963 (unpublished).

[50]R. J. Damburg and S. Geltman, Phys. Rev. Letters 20, 485 (1968).
[51]A. L. Fetter and K. M. Watson, Advan. Theoret. Phys. 1, 115 (1965).
[52]P. G. Burke, in *Scattering Theory: New Methods and Problems in Atomic, Nuclear, and Particle Physics*, edited by A. O. Barut (Gordon and Breach, New York, 1969), p. 193.
[53]G. W. F. Drake and M. Cohen, J. Chem. Phys. 48, 1168 (1968).
[54]A. L. Stewart, J. Phys. B 2, 309 (1969).
[55]E. G. Wikner and T. P. Das, Phys. Rev. 107, 497 (1957).
[56]M. Yoshimine and R. P. Hurst, Phys. Rev. 135, A612 (1964).
[57]Y. M. Chan and A. Dalgarno, Proc. Phys. Soc. (London) 85, 227 (1965).
[58]P. Sitz and R. Yaris, J. Chem. Phys. 49, 3546 (1968).
[59]G. W. F. Drake (private communication).
[60]G. W. F. Drake and A. Dalgarno, Astrophys. J. 157, 459 (1969).
[61]See, e.g., J. Callaway, R. W. LaBahn, R. T. Pu, and W. M. Duxler, Phys. Rev. 168, 12 (1968).
[62]M. H. Mittleman, Ann. Phys. (N.Y.) 14, 94 (1961).
[63]S. P. Khare and B. L. Moiseiwitsch, in Ref. 33, p. 49; Proc. Phys. Soc. (London) 85, 821 (1965).
[64]R. W. LaBahn and J. Callaway, Phys. Rev. 180, 91 (1969).
[65]S. Trajmar, D. G. Truhlar, and J. K. Rice, J. Chem. Phys. 52, 4502 (1970).
[66]A. R. Holt and B. L. Moiseiwitsch, J. Phys. B 1, 36 (1968).
[67]A. W. Weiss, J. Res. Natl. Bur. Std. 71A, 163 (1967).
[68]E. Clementi, IBM Technical Report No. 1965 (unpublished). Also, W. A. Goddard III (unpublished).
[69]R. P. Hurst, Acta Cryst. 13, 634 (1960).
[70]D. C. Cartwright and A. Kuppermann, Phys. Rev. 163, 86 (1967).
[71]C. L. Pekeris, Phys. Rev. 115, 1216 (1959).
[72]W. A. Goddard, Phys. Rev. 157, 81 (1967); 172, 7 (1968); J. Chem. Phys. 48, 400 (1968); 48, 1008 (1968); W. J. Hunt and W. A. Goddard, Chem. Phys. Letters 3, 414 (1969).
[73]C. L. Pekeris, Phys. Rev. 126, 143 (1962).
[74]W. Kolos and K. Pecul, Ann. Phys. (N.Y.) 16, 203 (1961).
[75]K. L. Bell, D. J. Kennedy, and A. E. Kingston, J. Phys. B 2, 26 (1969).
[76]B. Schneider, Phys. Rev. A 2, 1873 (1970). The authors thank Dr. Schneider for providing a copy of this work prior to publication.
[77]S. P. Khare and P. Shobha, in Ref. 37, p. 844.
[78]A. H. Gabriel and D. W. O. Heddle, Proc. Roy. Soc. (London) A258, 124 (1960).
[79]R. M. St. John, F. L. Miller, and C. C. Lin, Phys. Rev. 134, A888 (1964).
[80]E. N. Lassettre, J. Chem. Phys. 43, 4479 (1965).
[81]D. G. Truhlar, J. K. Rice, S. Trajmar, and D. C. Cartwright, Chem. Phys. Letters 9, 299 (1971).
[82]J. K. Rice, D. G. Truhlar, D. C. Cartwright, and S. Trajmar, Sandia Laboratories Research Report No. SC-RR-710474, 1971 (unpublished).
[83]J. K. Rice, A. Kuppermann, and S. Trajmar, J. Chem. Phys. 48, 945 (1968).
[84]A. Kuppermann, J. K. Rice, and S. Trajmar, J. Phys. Chem. 72, 3894 (1968).
[85]J. K. Rice, Ph. D. thesis (California Institute of Technology, 1969) (unpublished).
[86]K. J. Miller, S. R. Mielczarek, and M. Krauss, J. Chem. Phys. 51, 26 (1969).
[87]As an example of the application of this method, see S. Trajmar, J. K. Rice, P. S. P. Wei, and A. Kuppermann, Chem. Phys. Letters 1, 703 (1968).
[88]Reference 3, pp. 325–326.
[89]L. I. Schiff, *Quantum Mechanics*, 2nd ed. (McGraw-Hill, New York, 1955), pp. 169–170. We thank S. Lipsky for helpful discussions on this point.